The Dissertation Committee for Kelly Ann Hereid Certifies that this is the approved version of the following dissertation:

El Niño-Southern Oscillation Variability during the Little Ice Age and Medieval Climate Anomaly Reconstructed from Fossil Coral Geochemistry and Pseudoproxy Analysis

Committee:

Terrence Quinn, Supervisor

Timothy Shanahan

Frederick Taylor

Charles Jackson

Ginny Catania

El Niño-Southern Oscillation Variability during the Little Ice Age and Medieval Climate Anomaly Reconstructed from Fossil Coral Geochemistry and Pseudoproxy Analysis

by

Kelly Ann Hereid, B.A.

Dissertation

Presented to the Faculty of the Graduate School of

The University of Texas at Austin

in Partial Fulfillment

of the Requirements

for the Degree of

Doctor of Philosophy

The University of Texas at Austin

December 2012

El Niño-Southern Oscillation Variability during the Little Ice Age and Medieval Climate Anomaly Reconstructed from Fossil Coral Geochemistry and Pseudoproxy Analysis

Kelly Ann Hereid, Ph.D

The University of Texas at Austin, 2012

Supervisor: Terrence M. Quinn

The El Niño-Southern Oscillation (ENSO) dominates global interannual climate variability. However, the imprint of anthropogenic climate change hinders understanding of natural ENSO variability. Model predictions of the response of future ENSO variability to anthropogenic forcing are highly uncertain. A better understanding of how ENSO operates during different mean climate states may improve predictions of its future behavior.

This study develops a technique to quantify the response of tropical Pacific sea surface temperature and salinity to ENSO variations. This analysis defines expected regional relationships between ENSO forcing and the tropical Pacific climate response. For example, the western tropical Pacific records El Niño events with greater skill than La Niña events; whereas the oceans near the South Pacific Convergence Zone (SPCZ) preferentially record La Niña events. This baseline understanding of regional skill

calibrates interpretations of both modern and pre-instrumental coral geochemical climate proxy records.

A suite of monthly resolved $\delta^{18}O$ variations in a fossil corals (*Porites* spp.) from the tropical western Pacific (Papua New Guinea) and the SPCZ (Vanuatu) are used to develop case studies of ENSO variability under external forcing conditions that differ from the modern climate. A record from Misima, Papua New Guinea (1411-1644 CE) spans a period of reduced solar forcing that coincides with the initiation of the Little Ice Age. This record indicates that the surface ocean in this region experienced a small change in hydrologic balance with no change in temperature, extended periods of quiescence in El Niño activity, reduced mean El Niño event amplitudes, and fewer large amplitude El Niño events relative to signals captured in regional modern records. Several multidecadal (~30-50 year) coral records from Tasmaloum, Vanuatu during the Medieval Climate Anomaly (~900-1300 CE), a period of increased solar forcing, depict ENSO variability that is generally lower than modern times. However, these records often cannot be distinguished from 20th century ENSO variability due to ENSO variability uncertainty associated with record lengths. Neither record can be tied to concurrent changes in solar or volcanic forcing, calling into question the paradigm of ENSO variability being predominantly mediated by external forcing changes on multidecadal time scales.

Table of Contents

Introduction

The El Niño-Southern Oscillation (ENSO) is the largest source of interannual climate variability on the planet. The substantial human impacts of this climate phenomenon encompass droughts, fires, flooding, and fishery collapse. As one of the largest drivers of climate variability on human timescales, it is critical to understand how that variability might change in response to future climate changes, particularly anthropogenic global warming.

Extensive modeling efforts have attempted to predict future changes in ENSO variability, but ENSO in the modern climate is one of the largest sources of inter-model uncertainty, as its physical drivers and dynamical initiation remain poorly understood (Collins et al., 2010). Plausible physical mechanisms exist that would strengthen ENSO activity in response to warming, such as weakening Walker circulation (Vecchi and Soden, 2007); however, this atmospheric circulation change may be partly or completely offset by changes in ocean circulation, such as the ocean thermostat mechanism (Clement et al., 1996). Depending on the specific details of model parameterization, future ENSO predictions vary from strengthening to weakening ENSO variability, with an increased bias towards either El Niño or La Niña event initiation (Figure I.1).

The instrumental record could provide some insight into how the ENSO system has behaved in the past, as spatial patterns of sea surface temperature (SST) and salinity (SSS) changes provide readily identifiable markers of ENSO events. However, these

records do not extend prior to the late 19th century for SST, or approximately 1950 for SSS, and they dramatically improve in quality and spatial coverage only in the last several decades (1950-present for SST, 1970-present for SSS) (Delcroix et al., 2011; Rayner et al., 2003). Unfortunately, this period coincides with significant increases in anthropogenic forcing in the atmosphere, so it is unclear whether the variability that occurs in this period reflects natural variations in the ENSO system or a perturbed climate state.

Due to the limitations of model and instrumental data, we chose to focus on paleoclimate proxies from the pre-instrumental period. However, ENSO is a particularly difficult problem to approach using paleoclimate proxies. Resolution of at least one year is required to resolve individual ENSO events, since ENSO events are tied to the annual cycle, and the largest anomalies associated with events are predominantly located in remote regions of the Pacific Ocean. Given these limitations, we selected coral geochemistry as a paleoclimate proxy. Corals record changes in SSS ($\delta^{18}O$) and SST (Sr/Ca and $\delta^{18}O$), which are both strongly influenced by ENSO; they grow in regions that experience large ENSO-driven climate anomalies; and precise dating techniques and density banding permit seasonal resolution or better (eg., Cole et al., 1993).

This research consists of three case studies. We begin in the modern climate, using a combination of a forward model of instrumental pseudoproxy data and a suite of published modern coral records to set the expectation for how different regions of the Pacific might be expected to respond to ENSO events, in terms of both overall skill at

selecting known ENSO events, as well as potential biases towards recording either El Niño or La Niña events. After constraining the modern climate response to ENSO variability, we use a suite of fossil coral records from the western tropical Pacific to bracket the range of natural climate variability in the late Holocene. The Little Ice Age (LIA), a time period of known reductions in external forcing through both reduced solar activity and enhanced volcanism (Steinhilber et al., 2012), has an uncertain impact on tropical mean climate state, and its effect on interannual variability is correspondingly poorly constrained. Similarly, the Medieval Climate Anomaly (MCA) is a period of enhanced solar activity (Steinhilber et al., 2012), but the paucity of tropical paleoclimate records from this interval limits our understanding of its impact on mean tropical climate state and interannual variability.

This research has uncovered previously unexamined variations in proxy skill and bias that are critical to comparing proxy reconstructions from different regions, as is common in multiproxy reconstructions. Utilizing this new information, we find that the LIA experienced a broad, century-scale decline in El Niño activity (but do not interpret La Niña variability given the location of the proxy). Records from the MCA suggest the possibility of slightly less ENSO variability relative to modern times as well, but uncertainties in this period are larger due to the length of the available records. However, neither of these suites of pre-industrial coral records appears to be directly driven by mean state change on at least multidecadal time scales. Concurring with recent modeling work (Wittenberg, 2009), we find that mean climate state on sub-centennial time scales is

not clearly tied with ENSO variability, which may explain the large uncertainties associated with modeling future ENSO variability in GCM's.

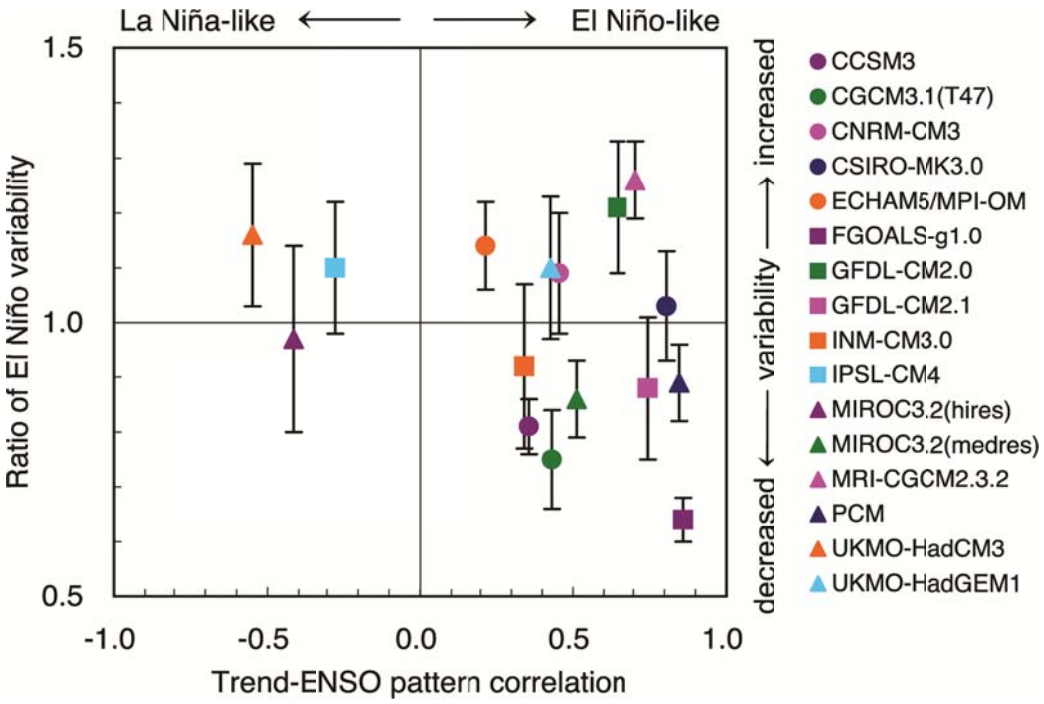

Figure I.1. Model projections of ENSO response to future climate change. ENSO is a major source of uncertainty in projections of future climate change, with the potential for either increased or decreased ENSO variability, with a stronger bias towards either El Niño or La Niña events **(**IPCC AR4, 2007, Fig. 10.16).

Chapter 1: Assessing spatial variability in ENSO event detection skill using coral geochemistry

Kelly A. Hereid[1,2], Terrence M. Quinn[1,2], Yuko M. Okumura[2]

[1]Department of Geological Sciences, Jackson School of Geosciences, University of Texas, Austin, Texas 78705, USA

[2]Institute for Geophysics, Jackson School of Geosciences, University of Texas, Austin, Texas 78758, USA

* Chapter 1 has been accepted in a revised form in Paleoceanography.

ABSTRACT

The El Niño-Southern Oscillation (ENSO) drives interannual climate variability, but evidence of its pre-instrumental expression is limited to proxy data and model inference. We develop a skill assessment technique using instrumental records of sea surface temperature (SST) and salinity (SSS), and apply it to a suite of 23 coral $\delta^{18}O$ records, a common ENSO proxy. We compare coral proxy skill with pseudoproxy records constructed from instrumental data to establish the expected proxy response to ENSO events and constrain proxy sensitivity. The central Pacific has a balanced response towards ENSO events, the Western Pacific Warm Pool (WPWP) favors El Niño expression, and the South Pacific Convergence Zone (SPCZ) preferentially records La Niña events. Eastern Pacific coral records display a surprisingly low ENSO sensitivity despite the presence of large ENSO-related SST anomalies, suggesting non-climatic influences on several coral records from this region. Networks of proxy data skill ratings

may better delineate the spatial structure of the ENSO response, a feature of the climate system that is currently poorly reproduced in climate models.

INTRODUCTION

ENSO events in the instrumental period are robustly defined using consistent methodologies (Ashok et al., 2007; Larkin and Harrison, 2005; Trenberth, 1997; Trenberth and Tepaniak, 2001), but long-term data trends and the wide range of climate parameters recorded by proxies have long hampered the development of consistent proxy ENSO definitions. ENSO activity quantification techniques vary widely in proxy records, and include symmetrical thresholds related to standard deviation (Cobb et al., 2003; McGregor et al., 2010; Stahle et al., 1998), change in standard deviation (Tudhope et al., 2001), sliding variance windows (D'Arrigo et al., 2005), reconstruction of SST fields (Evans et al., 2002; Wilson et al., 2006), and direct comparison with instrumental or historical timing of ENSO (Cole et al., 1993).

Each of these techniques has strengths and weaknesses that impact the fidelity of long-term ENSO reconstruction. Threshold choices are often subjective, especially far from the immediate Niño 3.4 index region, and assume a symmetrical response to El Niño and La Niña activity. Measures of total variability use arbitrary window sizes, and do not permit discrete ENSO event categorization, which is used in statistical analyses and direct comparison with historical records. SST field reconstructions require large proxy record datasets, and are sensitive to which records are included in the analysis. Direct comparisons tend to underemphasize false positive errors (events recorded in the

proxy but not in the instrumental record), and are difficult to extend beyond the past century.

We develop an empirically calibrated method to define ENSO activity that captures individual ENSO events and can be extended beyond the period of the instrumental and historical records. The method is tested using instrumental and reanalysis datasets of SST (Rayner et al., 2003) and SSS (Delcroix et al., 2011), as well as pseudoproxy data designed to mimic the response of coral $\delta^{18}O$ to changes in surface ocean conditions (Thompson et al., 2011). We then assess coral $\delta^{18}O$ records, which are a combined proxy for SST and SSS that captures ENSO and resolves individual events (Cobb et al., 2003; Cole et al., 1993; Correge, 2006; Evans et al., 2002; Gagan et al., 2000; Kilbourne et al., 2004). We utilize this method to locate high-skill proxy records, constrain coral sensitivity to ENSO variability, and analyze spatial biases in El Niño and La Niña event expression.

METHODS

We define modern instrumental ENSO events following the methodology of the NOAA/NWS/CPC Oceanic Niño Index (ONI), where the 3 month running mean of Niño 3.4 SST anomalies from NOAA ESRL (Rayner et al., 2003) exceed ±0.5°C for 5 or more consecutive overlapping seasons (Larkin and Harrison, 2005). We pad the beginning and end dates of each ENSO event by four months to account for standard coral age model uncertainty.

We band-pass filtered (2-8 year period) each record to isolate ENSO-dominated frequencies using wavelet analysis software (Torrence and Compo, 1998). This process removes the annual cycle, and since we only utilize the peak values from the filtered time series, we see no detrimental effects from interpolating annually resolved coral records. Filtering also removes long-term trends in the record, which obviates the need to change the threshold with mean variations, so the threshold can be extended beyond the instrumental record.

We select peaks from the filtered record to construct individual time series of potential ENSO events. We classify positive or negative excursions as El Niño or La Niña events based on the correlation between each record and Niño 3.4 SST anomalies. A positive correlation indicates that positive excursions correspond to El Niño events, and vice-versa. Using the record of filter peaks, we set the initial event detection threshold to 0.01 (psu for SSS, °C for SST, or ‰ for $\delta^{18}O$), and increase the threshold in step sizes of 0.01 through the full range of each record. At each step, we record any peaks that exceed the threshold, which we define as ENSO events for that particular threshold.

We optimize the threshold level for each individual record to minimize record errors. We compare the timing of ENSO events in Niño 3.4 (the control record) with that observed in the test record. We define two types of errors: 1) false positives, in which an event is identified in the test record, but not in the Niño 3.4 control record; and 2) false negatives, when a test record misses an ENSO event that is present in Niño 3.4 control record. In general, as the threshold level increases, the number of false positives

declines, which is eventually offset by increasing numbers of false negatives. The optimal threshold level for a given location occurs where the sum of both error types is minimized (Figure 1.S1). El Niño and La Niña threshold levels are optimized independently. If more than one potential threshold level reaches the minimum error level, we select the highest threshold level, so skill levels err on the conservative side. The threshold level determines record skill, defined as the percentage of all El Niño or La Niña events in the Niño 3.4 control record captured by the test record at the optimal threshold level.

To test whether the varying ENSO response in proxy data reflects a bias in proxy recording characteristics or real spatial variability in ENSO expression, we analyze ENSO detection skill using gridded SST data from HadISST (Rayner et al., 2003) and tropical Pacific SSS data (Delcroix et al., 2011). We calculate skill for 1° x 1° gridded SSS and SST data (Figure 1.1). SST and SSS variability at a reef site might be influenced by local variability that is not captured in the gridded datasets, but coral studies with in situ SST (DeLong et al., 2007) and SSS (Gorman et al., A coral-based reconstruction of sea surface salinity at Sabine Bank, Vanuatu from 1842-2007 CE, in revision at *Paleoceanography*, 2012) records demonstrate a close relationship between the local and gridded product. A simple forward model of "pseudoproxy" data (Thompson et al., 2011) shown in Equation 1 allows us to assess the competing isotopic influences of SST and SSS.

$$\delta^{18}O_{anom} = a_1 SST_{anom} + a_2 SSS_{anom} \qquad (1)$$

SST_{anom} and SSS_{anom} are calculated using instrumental SST data (Rayner et al., 2003) and instrumental SSS data (Delcroix et al., 2011). We assume a $\delta^{18}O$/SST relationship (a_1) of -0.22‰ per °C (Druffel, 1997). This leaves one unknown, the relationship between $\delta^{18}O$ and SSS (a_2), which has strong regional variations driven by local hydrology and water mass advection. We estimate a_2 in each grid cell (Figure 1.S2) based on a regression analysis of mean SSS (Delcroix et al., 2011) and a gridded dataset of ocean water $\delta^{18}O$ (LeGrande and Schmidt, 2006). Combining these pieces of data allows us to calculate a pseudoproxy $\delta^{18}O_{anom}$ value on a 1° x 1° grid, which provides an intermediary to directly compare the ENSO response expected from instrumental data with coral proxy skill. Error on the pseudoproxy skill (Figure 1.S3) derives from the standard deviation of skill values at each grid box and the eight immediately surrounding grid cells (3° x 3°). Grid locations where the error exceeds the skill value should not be interpreted for ENSO variability.

We also assess ENSO detection skill of coral proxy records and to compare with the pseudoproxy. We include published coral records with at least annual resolution and more than 50 years of data (Table 1.S1), archived at the NOAA NCDC (http://www.ncdc.noaa.gov/paleo/paleo.html). Lower resolution records cannot resolve individual ENSO events, since ENSO is phase-locked to the annual cycle (Tziperman et al., 1994), and shorter records may oversample periods when ENSO was particularly active or quiescent, potentially skewing regional skill. Each record is linearly resampled to 12 samples per year.

RESULTS AND DISCUSSION

Instrumental and Pseudoproxy Records

Instrumental SST records from the central and eastern tropical Pacific have the most skill in capturing ENSO variability, with variable skill levels in the western Pacific, and a distinctive null zone between the two regions (Figure 1.1a, b). Instrumental SSS records are most skillful in capturing ENSO variability to the west of the Niño 3.4 region and under the South Pacific Convergence Zone (SPCZ, Figure 1.1c, d); this characteristic matches the pattern of peak precipitation anomalies during ENSO events (Delcroix et al., 2011; Okumura and Deser, 2010; Ropelewski and Halpert, 1987). The noisier SSS skill record is partly due to the relatively short period of high-quality SSS data (1970-2008). The SST and SSS spatial patterns do not always overlap, so the pseudoproxy analysis allows us to assess potential constructive or destructive influences on the combined SST and SSS signal. The pseudoproxy reconstruction predicts that the highest ENSO skill will be in the central and eastern tropical Pacific (Figure 1.1e, f).

An ideal proxy record would match the skill of the instrumental record in capturing ENSO variability. For example, a coral $\delta^{18}O$ record from a region where 70% of the El Niño events, as identified in the Niño 3.4 record, are captured in the local SST and SSS records should also capture 70% of El Niño events. Thus, the observed skill level estimated from the instrumental record sets the proper expectation for proxy skill at a given location. In reality, pseudoproxy records typically outperform a coral record at a given location. Coral proxies are expected to lose some percentage of that skill due to error accumulation (analytical and replication uncertainty, local variability not captured

in the gridded instrumental datasets, etc.), so the pseudoproxy typically records a slightly higher skill at the same location.

Coral Proxy Records

Pacific coral $\delta^{18}O$ records vary widely in their ability to skillfully record ENSO events (Figure 1.2a, b, Table 1.S2). Corals from the central tropical Pacific (CTP), Western Pacific Warm Pool (WPWP), SPCZ, and Indonesia regions generally record ENSO with a relatively high degree of skill (>40% El Niño skill). Corals from the eastern tropical Pacific and subtropical oceans outside of the SPCZ typically have El Niño event skill rates below 40%.

The low skill result from corals in the eastern tropical Pacific may in part reflect the paucity of coral records from this region. However, the coral records from the Galápagos Islands (Dunbar et al., 1994) and Secas Island (Linsley et al., 1994) both record less than 20% of El Niño or La Niña events. This result is unexpected because some of the largest ENSO-driven SST anomalies are found in the eastern tropical Pacific. We investigated this apparent discrepancy by applying the skill test to the instrumental pseudoproxies from the eastern Pacific. Although there is a limited amount of temporal overlap between the pseudoproxy record (1970-2008) and the coral records (Galápagos ends in 1953, Secas Island ends in 1984), the pseudoproxy evidence suggests that instrumental climate parameters outperform corals in this region. Pacific basin-wide estimates indicate that on average, the pseudoproxy outperforms a coral record at the same location by 11% (El Niño) and 3% (La Niña). However, we were surprised to find

that the pseudoproxy outperforms the Galápagos record by 76% (El Niño) and 75% (La Niña), and the Secas Island record by 69% (El Niño) and 58% (La Niña), which is the largest discrepancy between pseudoproxy and coral skill in the Pacific, and suggests a potential non-climatic bias. Additional coral records are needed to ascertain the cause of the observed discrepancy between the pseudoproxy and the two coral proxies from this region.

ENSO forcing frequently causes an asymmetric response in coral $\delta^{18}O$ records (Figure 1.2c). Although average El Niño and La Niña event skill is equivalent when the entire Pacific region is included (47% skill for El Niño events, 45% skill for La Niña events), the skill difference within individual records varies by up to 48% (mean skill difference: 17%). The CTP and WPWP regions of the tropical Pacific are home to the most skillful El Niño records, whereas the most skillful La Niña event records are primarily located in the CTP and SPCZ (Figure 1.2). Coral $\delta^{18}O$ records with greater than 40% El Niño skill and at most a 10% difference between El Niño and La Niña skill, reflecting balanced records with high skill, include Palmyra (Cobb et al., 2003), Kiritimati (Evans et al., 1998a), Vanuatu (Kilbourne et al., 2004), Madang (Tudhope et al., 2001), and Rarotonga (Linsley et al., 2004). Coral proxy records exhibit spatial skill biases, which must be constrained to appropriately compare records from different regions of the Pacific. The WPWP is strongly biased towards recording El Niño events, the surface ocean beneath the SPCZ predominantly records La Niña events, and the central Pacific experiences a balanced response to both El Niño and La Niña events

(Figure 1.2c), which is consistent with the pseudoproxy analysis. Therefore, coral records from the western tropical Pacific tend to record less total ENSO activity than CTP records from an identical time period. Lacking an awareness of spatial biases in proxy event expression may lead to varying estimates of ENSO activity based solely on incomplete spatial data coverage. However, combining records that isolate either El Niño or La Niña activity may improve our understanding of the relative contribution of each type of event to total ENSO variability over time.

We note that skill and threshold level are generally negatively correlated in the coral records, as lower threshold levels improve minor event capture ($r = -0.78$, El Niño; -0.77, La Niña). However, two notable exceptions are instructive. The eastern tropical Pacific has low threshold levels and low skill. Most interannual variability is driven by ENSO, leading to a low rate of false positives, but the region exhibits low overall ENSO sensitivity, leading to many missed events and a correspondingly low skill rating. The SPCZ has relatively high threshold levels, but high skill. While this region experiences more extratropical events relative to the CTP, ENSO events are strongly recorded due to the large salinity front associated with SPCZ migration. Therefore, the event selection thresholds are high enough to filter out local events, while missing very few ENSO events, which have a larger range of variability.

The coral skill reconstructions in this study inform proxy interpretations for proxy-model comparison work. The pseudoproxy-coral comparisons confirm, in most cases, that corals are sensitive recorders of local sea surface conditions, and in locations

where those sea surface conditions reflect ENSO-driven variability, corals provide robust long-term records of ENSO variability. However, the pseudoproxy forward model also provides a simple test for coral sensitivity, and records that fail this sensitivity test should not be included in training sets for model verification. This study also demonstrates that proxy records that are "ENSO-sensitive" actually encompass a wide range of ENSO responses depending on local SST and SSS conditions, and that these proxies might preferentially respond to either El Niño or La Niña events. Without an appropriate skill analysis, a model might train its total ENSO response on proxy records that only reflect a subset of ENSO events, or that preferentially record El Niño or La Niña events. However, incorporating networks of proxy data with their associated skill ratings may improve measures of the spatial structure of the ENSO response, a feature of the climate system that is currently a major source of discrepancies between instrumental data and climate models.

CONCLUSIONS

We compile a suite of instrumental, pseudoproxy, and coral proxy data to assess spatial variability in ENSO event capture. Skill ratings provide a means to directly compare instrumental and proxy ENSO responses through a pseudoproxy intermediary. Regions that capture ENSO in instrumental SST and SSS records do not necessarily overlap, so the pseudoproxy analysis shows where competing influences from SST and SSS lessen or enhance the expected proxy response. On average, El Niño and La Niña events appear in coral proxies with equal skill, but strong regional patterns favor one type

of event being recorded over the other at individual proxy locations. This improved understanding of the regional biases inherent in ENSO event expression delineates the limits of modern proxy interpretation, and will lead to improved interpretation of existing proxy records.

Future studies could utilize skill measures to assess the number of records needed to obtain adequate spatial coverage, similar to work done to reconstruct SST fields and ENSO variability from sparse coral and other proxy networks (Evans et al., 1998b, 2002; Wilson et al., 2010; Wilson et al., 2006). High skill, balanced proxy records in the CTP may be paired with proxy records that favor El Niño in the WPWP and La Niña proxy records in the SPCZ to construct a more robust understanding of spatial variability in ENSO expression prior to the instrumental record, which is critical for improving the spatial pattern of ENSO response in climate models. Targeting proxies in these high-skill regions limits the number of new records needed to gain a robust understanding of past ENSO variability, a significant consideration given the time and expense of generating new proxy records. Direct proxy quality measures may also improve multiproxy reconstructions of ENSO activity in the pre-instrumental era, as reconstructions may require fewer records from high-skill regions.

ACKNOWLEDGEMENTS

Financial support for the research was provided by the US National Science Foundation (OCE-1103430). We thank J. Emile-Geay for advice on data filtering, and constructive comments from the UT Stable Isotope Lab research group.

Chapter 2: Coral record of reduced El Niño activity in the early 15th to middle 17th century

Kelly A. Hereid[1,2], Terrence M. Quinn[1,2], Frederick W. Taylor[2], Chuan-Chou Shen[3], R. Lawrence Edwards[4], and Hai Cheng[4]

[1]*Department of Geological Sciences, Jackson School of Geosciences, University of Texas, Austin, Texas 78705, USA*

[2]*Institute for Geophysics, Jackson School of Geosciences, University of Texas, Austin, Texas 78758, USA*

[3]*Department of Geosciences, National Taiwan University, Taipei 106, Taiwan, ROC*

[4]*Minnesota Isotope Laboratory, Department of Geology and Geophysics, University of Minnesota, Minneapolis, Minnesota 55455, USA*

* Chapter 2 will be published in Geology in January, 2013. DOI: 10.1130/G33510.1

ABSTRACT

The El Niño-Southern Oscillation (ENSO) powers global interannual climate variability through changes in trade wind strength, temperature/salinity anomalies, sea level, and atmospheric circulation patterns. ENSO variability is well characterized in modern times, but instrumental records cannot fully describe natural ENSO variability due to the imprint of anthropogenic climate forcing. ENSO activity may also be affected by solar variability, but the response of ENSO to such changes is difficult to predict. We constructed a continuous, monthly resolved, spliced fossil *Porites* coral $\delta^{18}O$ and Sr/Ca record from Misima Island, Papua New Guinea, in the Western Pacific Warm Pool,

spanning 233 years (1411 – 1644 CE). The Misima coral record indicates that the surface ocean in this region experienced a small change in hydrologic balance with no change in temperature, extended periods of quiescence in El Niño activity and no change in average amplitudes of El Niño events relative to signals captured in regional modern records. The reduced El Niño variability occurs during a known change in solar forcing, the initiation of the Little Ice Age. However, there is no clear relationship between the timing of changes in solar forcing and ENSO activity, implying that ENSO variability changes arise from internal dynamics. The century-scale switch between active and inactive El Niño states has never previously been recorded, and provides a new baseline for climate models and reconstructions.

INTRODUCTION

The response of the tropical climate system to decreased solar forcing is debatable. The most recent period of reduced solar forcing is the Little Ice Age (LIA), ~1450–1850 (Steinhilber et al., 2009); some tropical paleoclimate records show LIA cooling (Thompson et al., 1995), but others indicate negligible temperature change (Hendy et al., 2002). Sediment and speleothem records suggest that a century-scale southward displacement of the Intertropical Convergence Zone and a weakened Asian Monsoon resulted in significant hydrologic reorganization during this interval (Oppo et al., 2009; Tierney et al., 2010; Zhang et al., 2008). The paleoclimate record of interannual variability is also unclear; records placing high levels of ENSO activity during the LIA

(Cobb et al., 2003) contrast with others where ENSO variability peaks during the Medieval Climate Anomaly (Moy et al., 2002).

Pre-industrial paleoclimate records can characterize the long-term response of ENSO variability to known natural perturbations in external forcing, providing an observational framework to inform predictions of the ENSO response to future climate change. This study assesses pre-industrial ENSO variability in the tropical western Pacific using a spliced, centennial-scale record (233 years) of monthly resolved coral-inferred sea surface temperature (SST) and salinity (SSS) during the early 15th to middle 17th century, a period coincident with the onset of the LIA (Steinhilber et al., 2009). We utilize oxygen isotope data ($\delta^{18}O$) as a combined proxy for SST and SSS (Cole et al., 1993; Evans et al., 2000), and Sr/Ca for age modeling and to constrain SST changes (Correge, 2006). This multi-proxy approach separates hydrologic changes from long-term temperature trends.

Misima Island, Papua New Guinea (PNG; 10.6°S, 152.8°E), lies at the southern edge of the Western Pacific Warm Pool (WPWP), an ocean region characterized by the warmest open-ocean surface temperatures, making it a major heat and moisture source to the climate system. The WPWP experiences cool (warm) and dry (wet) conditions during El Niño (La Niña) events (Rasmusson and Carpenter, 1982; Ropelewski and Halpert, 1987), and exhibits the ocean's largest SSS response to ENSO variability (Delcroix et al., 2011) (Figure 2.1). Regional precipitation and temperature anomalies during ENSO events have an additive effect on $\delta^{18}O$ in coral aragonite: large positive (negative)

excursions in $\delta^{18}O$ represent El Niño (La Niña) events (Quinn et al., 2006; Tudhope et al., 2001). We assess ENSO variability at Misima by calculating ENSO frequency and amplitude changes during the early 15th to middle 17th century, filling in a critical data gap in high-resolution pre-industrial climate records.

METHODS

Fossil and near-modern *Porites* coral heads were cored in beach storm deposits at Misima. Three-inch diameter cores were cut into 5-mm slabs and analyzed for diagenetic alteration using x-radiographs (Figure 2.S1) and scanning electron microscopy. Slabs that passed these screening criteria were micromilled along the maximum growth axis at approximately monthly resolution using a computer-assisted drilling stage. The data were linearly resampled to 12 samples per year. A composite time series was created using two spliced fossil cores.

Analytical precision is 0.05‰ for $\delta^{18}O$, and 0.02‰ for $\delta^{13}C$ (1σ, n = 393), with between-colony $\delta^{18}O$ uncertainty of 0.12‰ (Figure 2.S2). Analytical precision for Sr/Ca ratios is 0.015 mmol/mol (1σ), with between-colony uncertainty of 0.062 mmol/mol (1σ). Raw Sr/Ca measurements were corrected using internal standards (Schrag, 1999). The geochemical age model was shifted within error of the ^{230}Th dates (Table 2.S1) to match the timing of the 1578 El Niño event known from historical records (Ortlieb, 2000).

A band-pass filter applied to the coral time series (Figure 2.2) highlights variability at ENSO timescales (2–8 yrs). The filtered data error of ± 0.026‰ (1σ) was

determined using a Monte Carlo analysis of 1000 synthetic data sets consisting of the original data set with random, normally distributed inter-colony error added. A band-pass filter was applied to each synthetic data set; the average standard deviation at each data point reflects the uncertainty. Similarly, threshold uncertainty was estimated by calculating the threshold on 1000 synthetic filtered data sets with error included.

RESULTS

A significant median shift in coral $\delta^{18}O$ (–0.27‰, $p<0.0001$) between the fossil and near-modern Misima corals suggests warmer/fresher sea surface conditions in the early 15th to middle 17th century relative to the 20th century. The trend toward more negative isotopic values in modern times is observed in many coral records across the Pacific (Cobb et al., 2003; Hendy et al., 2002; Kilbourne et al., 2004). A portion of this shift at Misima may be due to intercolony variability, caused by local environmental variations (Linsley et al., 1999), but the deep thermocline and stable stratification in the WPWP tends to dampen upper water column variability (Lukas and Lindstrom, 1991). If this offset is due to regional climate trends, this finding is consistent with instrumental records indicating the WPWP is warming/freshening in response to climate change (Cravatte et al., 2009; Singh and Delcroix, 2011). The similar mean Sr/Ca values in the near-modern and fossil coral records imply little change in SST (Figure 2.S3), favoring the interpretation of a freshening trend as the mechanism driving coral $\delta^{18}O$ changes. However, instrumental SST data indicates that this region has warmed slightly since the period when the coral grew (28.18°C during coral growth period, 28.50°C in most recent

corresponding period, HadISST1.1). Furthermore, the annual cycle in coral $\delta^{18}O$ is significantly larger in the near-modern record than in the fossil (0.39‰ and 0.25‰, p = 0.0096), but statistically equivalent between the near-modern and fossil Sr/Ca records (0.119 mmol/mol and 0.104 mmol/mol, p = 0.3581), again suggesting a change in hydrology rather than a change in SST as the primary driver of the coral $\delta^{18}O$ variations.

The acquisition of a modern century-scale coral record from Misima, while ideal, has proven to be logistically unfeasible. Instead, the available near-modern Misima record was compiled with published PNG coral records to develop a modern calibration data set (Figure 2.S4, Table 2.S2). PNG records capture the full range of 20th century multidecadal ENSO variability (Quinn et al., 2006; Tudhope et al., 2001) and have a similar SSS response to ENSO events (Delcroix et al., 2011), making them suitable for direct century-scale comparisons with the fossil record at Misima. These regional records allow more suitable comparisons than the longer Palmyra fossil record, whose differing ENSO sensitivity limits comparisons between the two regions (Figure 2.S5). The Madang, Laing and Rabaul coral records have significantly greater interannual variance than the Misima fossil record ($p<0.0001$). The reduced interannual variability in the fossil Misima record relative to the century-scale modern PNG records suggests that ENSO was less active during the early 15th to middle 17th century.

DISCUSSION

To quantify variability changes using individual ENSO events, we compare each modern coral $\delta^{18}O$ record with the instrumental Niño 3.4 record to empirically determine

a threshold at which most ENSO events are captured, while minimizing incorrectly recorded events. To set the threshold for El Niño and La Niña events, we use a band-pass filter to remove long-term trends in individual records, and then incrementally change the threshold level in steps of 0.01‰. At each step, we record the number of accurately identified ENSO events, as well as the number of errors for each record, and set the ENSO event threshold where the sum of all errors is minimized. We modeled changes in error range with record length to calibrate the error to the length of the fossil record. From this analysis, we set a threshold for Misima El Niño events at a 0.11 ± 0.03‰ anomaly (Fig 2.2). The thresholds for La Niña events in this region are inflated by high rates of false positives (local, non-ENSO events); therefore, we only interpret changes in El Niño variability from PNG coral records. The accuracy rates for modern records from Laing and Madang are equivalent within error to the near-modern Misima record, but the accuracy at Rabaul does not overlap the near-modern Misima record, so it is excluded from further discrete event capture analyses.

We applied the empirically determined El Niño threshold to the fossil Misima record. Fifteen El Niño events (10–25, ± 1σ) are observed over the 233-year fossil record. Using the same analysis, we found 15 El Niño events (10–22, ± 1σ) in the Madang record, 21 at Laing (16–24, ± 1σ), and 3 (2–4, ± 1σ) in the near-modern Misima record (Table 2.S3). We compare the fossil and modern records directly using 100 year running windows to count events (Figure 2.3). Events in the fossil record drop to as few as 3 El Niño events (2–6, ± 1σ) per century, below the minimum event counts per century

at Madang and Laing. The 117-year period between 1519 and 1636 CE contains fewer El Niño events per century than any century-long window in the modern Madang and Laing records. The fossil record also has a significantly lower number of total El Niño events than the century-scale modern records ($p = 0.0008$). The event number reduction does not represent a shift in the recurrence interval of El Niño events, but rather reflects long periods when the coral record experiences substantially reduced El Niño activity. The extended periods of quiescence in the late 16th and early 17th centuries drive an overall reduction in El Niño variability during this time, while the earlier section of the record contains a number of El Niño events comparable to modern times (Figure 2.3).

To quantify event magnitude changes, we calculated the amplitude peak for each El Niño event that crossed the event threshold for Madang, Laing, and Misima. We pooled the modern records and compared their magnitudes with the fossil record magnitudes. The modern median event size is 0.16‰ (0.14–0.19‰, 95% confidence interval), which is statistically equivalent ($p = 0.98$) to the fossil median event size of 0.16‰ (0.14–0.18‰, 95% confidence interval). This evidence shows that substantial changes in El Niño variability can occur even when event magnitudes remain consistent.

The reduced El Niño activity during the LIA at Misima could be explained two ways: either total ENSO variability in the Pacific is reduced in this interval, or there is an increase in La Niña events relative to El Niño events. Using only this WPWP record, we are unable to determine which of these scenarios is most likely, since this location is not expected to strongly record La Niña events. Therefore, we compare the Misima record

with the TexMex tree ring reconstruction of Niño 3 (D'Arrigo et al., 2005), which has a high-skill, balanced El Niño and La Niña response (63% El Niño/67% La Niña). To assess the relative strength of El Niño versus La Niña events, we calculate a 30-year running mean of the ratio of El Niño to La Niña event number. This record captures a broad decline in the proportion of El Niño events centered near 1600 CE (Figure 2.4). Based on this analysis, we cannot exclude an increase in the proportion of La Niña events relative to El Niño events as a possible explanation for the decline in El Niño events at Misima.

Two competing hypotheses predict how ENSO variability reacts to a change in forcing. Previous studies suggested that extended periods of low ENSO variability could reflect a La Niña-like state, with a high zonal gradient in the Pacific damping the initiation of El Niño events (Mann et al., 2005). The response to an decline in solar input is offset by reduced upwelling in the eastern equatorial Pacific (Clement et al., 1996), causing a decrease in zonal Pacific SST gradient that is directly related to solar forcing, which favors El Niño event initiation (Emile-Geay et al., 2007). This effect is countered by increased zonal atmospheric circulation and deepening of the WPWP thermocline in response to cooling (Vecchi and Soden, 2007), so it is not clear which process would dominate. These two viewpoints may not be reconcilable within the limited time frame of models or the instrumental record, as the time required for the ENSO system to respond to a change in mean state is on the order of several centuries (Stevenson et al., 2012; Wittenberg, 2009). The reduced El Niño activity over the period of reduced solar forcing

in the fossil Misima record appears to support the latter hypothesis, but a direct comparison with solar variability suggests that solar forcing alone is inadequate to explain multidecadal changes in interannual variability (Figure 2.S6). Rather, multidecadal variability changes in the Misima fossil coral record fall within the range of unforced internal variability predicted by modeling studies (Wittenberg, 2009). Additional long, annually resolved paleoclimate records are essential to assess more realizations of changes in incoming solar radiation and determine how mean state changes influence ENSO variability.

CONCLUSIONS

The multi-century fossil record of El Niño variability at Misima suggests sizeable El Niño system changes during a period of tropical hydrologic changes in the early 15th to middle 17th century. The change in the mean and amplitude of the annual cycle in coral $\delta^{18}O$, without attendant Sr/Ca changes, is consistent with the concept that the WPWP underwent small but significant salinity changes without a corresponding change in SST between the early 15th to middle 17th century and modern times. The reduction of interannual variability depicts a climate state in which El Niño variability was significantly reduced relative to modern times, which occurs despite equivalent El Niño event magnitudes. This altered variability reflects periods of El Niño quiescence interspersed with times when El Niño variability approaches modern conditions, with no clear connection to solar forcing. This study demonstrates that significant changes in

interannual variability are possible despite only minimal changes in mean climate state as a result of unforced internal variability.

ACKNOWLEDGEMENTS

We thank J. Banner for access to ^{230}Th dating facilities at UT. J. Emile-Geay provided valuable advice on filtering techniques. We also appreciate constructive suggestions from C. Jackson, T. Shanahan, and the UT Stable Isotope Lab research group. This work was supported by the US National Science Foundation (OCE-0202549, OCE-042349, OCE-0401810, OCE-0742217) and the University of Texas (Jackson School of Geosciences, Institute for Geophysics Ewing-Worzel Fellowship). Geochemical data will be available at the National Climatic Data Center (http://www.ncdc.noaa.gov/paleo/paleo.html). Correspondence and requests for materials should be addressed to K.A.H. (hereidk@utexas.edu).

Chapter 3: Assessing changes in mean climate and ENSO variability using multidecadal coral records from the Medieval Climate Anomaly

Kelly A. Hereid[1,2], Terrence M. Quinn[1,2], Frederick W. Taylor[2], Chuan-Chou Shen[3], R. Lawrence Edwards[4], and Hai Cheng[4]

[1]*Department of Geological Sciences, Jackson School of Geosciences, University of Texas, Austin, Texas 78705, USA*

[2]*Institute for Geophysics, Jackson School of Geosciences, University of Texas, Austin, Texas 78758, USA*

[3]*Department of Geosciences, National Taiwan University, Taipei 106, Taiwan, ROC*

[4]*Minnesota Isotope Laboratory, Department of Geology and Geophysics, University of Minnesota, Minneapolis, Minnesota 55455, USA*

* Chapter 3 is in preparation for publication

ABSTRACT

The El Niño – Southern Oscillation (ENSO) drives global interannual variability, with widespread economic and societal impacts. As one of the most important climate phenomena to occur on human timescales, it is critical to constrain the range of potential future changes. Given the limitations of the instrumental record, we must rely on proxy records, but these records are often short and discontinuous. Although short fossil records may be statistically distinguishable from modern records if the change in ENSO variability is dramatic, the limited number of ENSO event realizations in multidecadal records requires cautious interpretation. We utilize a pair of multidecadal coral oxygen

isotope records from the Medieval Climate Anomaly (MCA) to assess the extent of changes in ENSO variability in response to a period of increased solar forcing, as well as to address the uses and limitations of short proxy records. We find no evidence for a shift in mean $\delta^{18}O$ or seasonal cycle during the MCA relative to modern records. ENSO activity in the Medieval Climate Anomaly is generally reduced relative to modern times, but portions of the dataset cannot be distinguished from modern datasets due to uncertainty associated with the record length. Multidecadal proxy records require dramatic changes in ENSO variability to be distinguished from modern centennial-scale records.

INTRODUCTION

The El Niño-Southern Oscillation (ENSO) is the largest source of interannual climate variability on the planet. However, the sensitivity of this climate variation to changes in mean climate state is poorly constrained. The instrumental record lacks enough realizations of multidecadal variability to determine if recent changes in ENSO activity are a response to a changing climate, or are within the natural range of variability of the climate system. Furthermore, the instrumental period coincides with significant anthropogenic atmospheric forcing, limiting reconstructions of natural variability. Therefore, we utilize paleoclimate records during periods with known changes in external forcing to constrain the range of natural variability in the ENSO system. Given the limited understanding of how ENSO will respond to future climate changes, we utilize

fossil coral $\delta^{18}O$ proxy data to examine changes in ENSO variability during the Medieval Climate Anomaly (MCA), a previous period of increased external forcing.

The MCA is best defined in the North Atlantic region; its timing and occurrence are debated in the tropics. Although a small change in solar forcing is clear (Steinhilber et al., 2012), it is less certain if the deep tropics reacted with a change in mean temperature or hydrologic state. Tree ring and coral records available in this period suggest a trend towards cooler and/or drier conditions in the central and eastern tropical Pacific (Cobb et al., 2003; Cook et al., 2004; Li et al., 2011) during this time period. Pairing these records with evidence for an increased tropical Pacific zonal sea surface temperature (SST) gradient during this time interval (Conroy et al., 2010; Conroy et al., 2009; Oppo et al., 2009) would indicate conditions that would be more favorable to initiating La Niña events. However, this contradicts the expected weakened Walker circulation in response to increased external forcing described in climate models (Vecchi and Soden, 2007), which would generally favor El Niño event initiation.

This record includes two fossil coral records that grew during the MCA from Tasmaloum, Vanuatu (15.6°S, 166.9°E). Vanuatu is located beneath the South Pacific Convergence Zone (SPCZ). The position of the SPCZ and its associated precipitation band and advection front is controlled by ENSO events on interannual time scales. Consequently, climate variability at Vanuatu is dominated by changes in sea surface salinity (SSS) on an interannual time scale. This site experiences cool (warm) and dry (wet) conditions during El Niño (La Niña) events (Figure 3.1). Corals are sensitive to

changes in SST and SSS associated with ENSO (Cobb et al., 2003; Cole et al., 1993; Correge, 2006; Crowley et al., 1999; Evans et al., 2002; Fairbanks et al., 1997; Linsley et al., 2000; Quinn and Sampson, 2002; Tudhope et al., 2001; Urban et al., 2000), and SST and SSS anomalies during ENSO events at this location are additive in $\delta^{18}O$, so coral records from this region exhibit robust ENSO variability (Kilbourne et al., 2004). Modern proxy records in this region show a balanced response to El Niño and La Niña activity, making Vanuatu well-suited to reconstructing total ENSO variability through time (Hereid et al., in revision, 2012).

METHODOLOGY

Porites coral cores were collected from storm deposits and uplifted terraces at Tasmaloum, Vanuatu, at the south end of the main island of Espiritu Santo, and cut into 5mm slabs. Each slab was screened for diagenetic alteration using x-radiographs. Cores that passed the screening criteria were drilled at approximately monthly resolution using a computer-assisted drilling stage.

Isotopic analyses were conducted at the Stable Isotope Lab at the University of Texas at Austin. A portion of the samples were analyzed on a Thermo-Finnigan MAT 253 Dual-inlet gas source isotope ratio mass spectrometer (IRMS) with attached Kiel IV carbonate preparation device. The remaining samples were analyzed on a Delta V with attached GasBench and ConFlo. Internal standards testing confirms that isotopic values are consistent between the two instruments. The analytical precision was determined

using repeated measurements of the NBS-19 and CM standards in each instrument run (0.06‰, 1σ, n = 268).

Cores were ^{230}Th dated on a Finnigan MAT Element inductively coupled plasma mass spectrometer (ICP-MS) at the University of Minnesota Isotope Laboratory. Age models were constructed using annual cycles in geochemistry, with the coldest month assigned to August and the warmest to February based on modern instrumental mean climatology.

The replication error (0.15‰) is constructed using the overlapping time interval (1928-1992 CE) between the modern Malo Channel (Kilbourne et al., 2004) and Sabine Bank (Gorman et al., in review, 2012) Vanuatu coral records, and reflects the mean absolute value of the difference between the two records at each monthly time step. The filtered data error (±0.03‰, 1σ) was calculated using a Monte Carlo simulation (1000 iterations) with replication error randomly added to the original dataset. The new synthetic dataset was filtered, and the average standard deviation at each data point reflects the uncertainty.

We selected ENSO events from the filtered record following the technique of (Hereid et al., in revision, 2012). This is a calibration technique based on a comparison between the modern coral records and the Niño 3.4 index, which is used to empirically determine El Niño and La Niña event thresholds. Since the filtering technique removes low-frequency variability from the record, these thresholds can then be applied to pre-instrumental records that may have undergone changes in mean climate state. El Niño

and La Niña thresholds are determined independently, and reflect the mean thresholds chosen by a Monte Carlo analysis (1000 iterations) that incorporates replication error.

RESULTS AND DISCUSSION

Mean Climate State

We recovered 31 year and 53 year sections of monthly-resolved coral $\delta^{18}O$, dating to the MCA (Figure 3.2). The mean for the 53 year record is -4.93‰, and the record standard deviation is 0.18‰. The 31 year record mean is -4.90‰, with a similar level of variability at 0.22‰. Given a mean value of -4.86‰ (standard deviation 0.21‰) at Malo Channel, and -4.81‰ (standard deviation 0.24‰) at Sabine Bank, it appears that mean values have remained relatively consistent between the MCA and the modern records. However, these mean values reflect climate conditions over widely varying periods of time. Furthermore, the mean values give no estimate of uncertainty associated with between-colony replication error. Therefore, to make direct comparisons among the proxy records, we need a way to directly assess the impact of record length, as well as simulate the range of uncertainty driven by replication error.

We calculated mean variability associated with differences in record length using the longest modern record from Vanuatu: Sabine Bank, which is 165 years in length. For sections of the record ranging in length from one month to the total length of the record, we selected a random starting place, added random, normally distributed replication uncertainty (±0.15‰), and calculated the mean. This process was repeated for 1000 iterations, to assess the impact of both replication uncertainty and record length on mean

uncertainty (Figure 3.3). This model predicts that the fossil 31 year record (mean -4.90‰) has a mean error (1σ) of ±0.10‰, the fossil 53 year record (mean -4.93‰) has a mean error of ±0.07‰, the Malo Channel record (mean -4.86‰) has a mean error of ±0.07‰, and the Sabine Bank record (mean -4.81‰) has a mean error of <0.01‰ (which reflects only replication uncertainty) (Figure 3.4). However, since we have more than one section of proxy record available during the MCA, we can combine those two records to get a fossil mean value of -4.92‰. Randomly selecting two sections from the modern records equal in length to the fossil records gives a mean error of ±0.06‰. We also note that the Sabine Bank record contains a substantial trend through time; the mean of the time period overlapping the Malo Channel record is -4.91‰. Functionally, this analysis demonstrates that the mean $\delta^{18}O$ values of the MCA and modern coral records are statistically indistinguishable, which implies that overall climate conditions between these two periods were similar. However, the error associated with multidecadal records when calculating century-scale mean values may be substantial, but can be reduced by combining multiple periods in time.

Annual Cycle

Previous authors have hypothesized that there may be a link between changes in ENSO variability and changes in the magnitude of the annual cycle in the tropical Pacific (Koutavas, 2009). Corals are one of a limited subset of proxy records that can resolve the amplitude of the annual cycle, so we utilize seasonal means to assess potential annual cycle variations. For each fossil and modern record, we calculate the 3-month average

$\delta^{18}O$ value for each year during the months surrounding the minimum and maximum values in the $\delta^{18}O$ climatology of each record. This seasonal range allows us to compare distributions of variability in the annual cycle.

We group the fossil and modern records together to directly compare the two time periods. Since it is not clear what water depth the fossil corals experienced as they grew, we attribute between-core differences in the same time period to site-dependent differences in annual cycle. The mean seasonal cycle in the fossil coral $\delta^{18}O$ records is 0.26‰ (±0.14‰, 1σ), and in the modern coral records is 0.28‰ (±0.15‰, 1σ). Neither the mean nor the variance differences are significantly different. The equivalent means demonstrate that the overall amplitude of the annual cycle has not varied between the study intervals. The equivalent variances suggest that interannual variability has remained consistent as well, as ENSO variability is the major contributor to short-term variations in the annual cycle.

ENSO Variability

We applied an empirically calibrated threshold of 0.10 ± 0.03‰ for El Niño events and –0.11 ± 0.03‰ for La Niña events to the filtered modern and fossil coral $\delta^{18}O$ records. These thresholds were determined by calculating the mean coral $\delta^{18}O$ value for the overlapping time interval of the two modern records (1928-1992). We then add random replication uncertainty (1000 iterations), calculate the threshold in each iteration, and use the mean and standard deviation of thresholds over the entire simulation. Comparisons between the modern records and instrumental data using the Monte Carlo

simulation indicate a skill rating for this region of 60 ± 10% (1σ) for El Niño events, and 55 ± 15% (1σ) for La Niña events. In the combined modern records, we find 0 false positive (excess) El Niño events, 3 false positive La Niña events, 7 false negative (missed) El Niño events, and 7 false negative La Niña events. Although El Niño and La Niña events have comparable skill ratings in this region, La Niña event definitions are more sensitive to the choice of threshold, so we have higher confidence in the skill ratings of El Niño events at Vanuatu.

It is difficult to directly compare long-term ENSO event rates in records of different lengths, so we employ a variety of techniques to analyze subsets of the modern records that are equivalent in length to the fossil coral sections. To assess the impact of record length on the ability to define ENSO events, we conducted a Monte Carlo simulation using the modern Sabine Bank record during the period in which it overlaps the instrumental record. We select segments ranging in length from 30 years (approximately the time scale of multidecadal ENSO variability) to the entirety of the record, add replication uncertainty, and calculate the thresholds utilizing only that particular segment (1000 iterations). Although the mean skill values are equivalent within uncertainty whether the threshold is calculated on the entire record or using multidecadal sections, the variability in skill is strongly dependent on record length. In this region, a 30-year record may deviate from a centennial-scale skill rating by up to ~20%. Therefore, if only a 30-year fossil segment is available, and El Niño skill in long modern records is approximately 60%, we could not differentiate records reflecting anywhere from 40-80%

El Niño skill. In practice, this means that very large changes in ENSO variability would be necessary to distinguish short fossil records from centennial-scale modern calibration records.

The simplest event count comparison technique is a running event count, in which we count the number of El Niño or La Niña events in a running window equivalent in length to the fossil sections, which preserves the multidecadal ENSO variability present in the modern records. We find that there are periods of the modern records that are similar to some of the fossil ENSO event counts, but in general, the fossil records have slightly reduced ENSO event counts (Figure 3.5).

To better quantify the likelihood of randomly reproducing the fossil records if ENSO activity remained the same as modern activity, we use a modified bootstrap analysis. From each modern record, we select a random assortment of years equal in number to the length of a given fossil record (where each year can only be selected once). This generates a new "pseudofossil" record, with a number of El Niño or La Niña events corresponding to the years selected from the modern record. By repeating this process 10,000 times, we generate a distribution of possible ENSO event counts for both a 31 and 53 year record from the modern Malo Channel and Sabine Bank modern Vanuatu coral records. We calculate the percentage of event counts that are less than or equal to the actual fossil event counts to place a confidence level on the difference between modern and fossil event rates. Again, we find that in some instances, the fossil records fall within

the potential distribution of modern events, but there are also cases where the fossil records experience less ENSO activity than the modern records (Figure 3.6).

Implications for MCA Climate

The multidecadal fossil coral records we analyzed from the MCA show striking similarities with the modern records from Vanuatu. The similarities in mean state, seasonal cycle, and ENSO variability all suggest that the climate of the tropical Pacific in modern times is currently within the range of natural variability for the region. This analysis shows that although multidecadal slices of time such as those recorded by the fossil corals in this study may not be able to distinguish the centennial-scale trends found in long modern records, these shorter records do permit tests of whether modern records exceed the bounds of regional natural variability. Furthermore, combining multiple short proxy records reduces the total uncertainty associated with sampling intervals on the same scale as multidecadal variability in the Pacific. Since coral proxies of this age rarely exceed a few decades in length, this approach of incorporating a series of discontinuous proxy pieces may improve future climate assessments.

CONCLUSIONS

Using an event detection algorithm and statistical techniques that maximize the utility of short fossil records, we find limited differences in mean climate state and the mean annual cycle between the MCA and the present. El Niño and La Niña activity during the MCA at Vanuatu is somewhat less active than modern ENSO activity levels; however, the limited number of event realizations prevents the 31 year record from being

statistically distinguished from modern event rates. This suggests that very large climate changes would need to occur for shifts to be resolved in a record of this length. The 53 year record shows some changes in ENSO variability relative to the modern records, but again shows substantial overlap with modern variability. However, the techniques we utilize to combine a suite of discontinuous periods of time may be able to paint a more representative picture of long-term mean climate and ENSO variability changes in the tropical Pacific.

Conclusion

In this dissertation, a new set of techniques was developed to quantitatively define the skill of modern coral-based climate records to capture the surface ocean response to ENSO forcing. A simple forward model predicts the oxygen isotopic response in the coral skeleton to changes in sea surface temperature (SST) and sea surface salinity (SSS). This gridded pseudoproxy product permits predictions to be made regarding how a coral proxy would perform at any given location using an empirically calibrated ENSO analysis technique that selects an optimal threshold to quantify El Niño and La Niña events. Moreover, actual coral records were compared to the pseudoproxy to isolate instances when the coral underperforms relative to the expectation based on instrumental data. This result allows the assessment of which coral records are strongly impacted by non-climatic factors; such records may lead to conflicting interpretations when incorporated into broader climate analyses, such as multiproxy reconstructions.

The empirical skill calibration technique developed in the pseudoproxy was then applied to a suite of modern coral records to assess the spatial expression of ENSO events over the 20th century. Since El Niño and La Niña events are calculated independently, we can determine which regions of the Pacific experience a greater expression of each event type. While central Pacific coral proxies record El Niño and La Niña events with approximately equal skill, coral proxies from the Western Pacific Warm Pool (WPWP) predominantly records El Niño events, and coral proxies from the South Pacific Convergence Zone (SPCZ) predominantly records La Niña events. These patterns must

be taken into account when directly comparing any proxies from different areas, as inconsistent ENSO expression through time may simply reflect preferential recording of different types of events in different regions.

Having set the expectation for how ENSO should be recorded by corals in the modern setting, two case studies assessed how ENSO variability might change in response to changes in mean climate state. Currently, climate models express a wide range of disagreement as to how ENSO variability might react to future anthropogenic warming. Therefore, test cases were used to see how global climate has reacted to past changes in mean state, in hopes of providing a baseline for how the future climate might react. The first case study (Misima, Papua New Guinea) focused on ENSO variability during the Little Ice Age (LIA), a recent time period when surface temperatures have been reported to be cooler than modern (Steinhilber et al., 2012). The second case study (Tasmaloum, Vanuatu) focused on ENSO variability during the Medieval Climate Anomaly (MCA), a recent time period when surface temperatures have been reported to be warmer than modern (Steinhilber et al., 2012).

The coral $\delta^{18}O$ record from Misima, Papua New Guinea spans two centuries (1411-1644 CE) over the initiation of the LIA. This coral record predominantly reflects SSS variability, which is driven by El Niño activity at this site (Delcroix et al., 2011). El Niño activity shows a striking reduction that does not match any documented sources of external forcing, such as solar or volcanic variability, over the transition into the LIA. This suggests that ENSO variability on at least the multidecadal time scales recorded in

this study may be primarily driven by internal dynamics, and is not strongly susceptible to external climate forcing. However, during this transition, El Niño activity declined to an extent not seen in the instrumental record, which demonstrates that the full range of natural variability has not been captured in the instrumental period. The ability of ENSO to switch between highly active and minimally active phases of this duration has never previously been documented, and provides a new climate baseline to improve future climate models.

Two multidecadal sections of coral records from Tasmaloum, Vanuatu were used to assess ENSO variability during the MCA. These coral proxies record El Niño and La Niña variability with approximately equal skill, so can be used to assess changes in total ENSO variability. However, like many fossil coral records, they are relatively short in duration (~30-50 years), so experiments were also conducted to assess the error introduced due to record length. Mean climate, seasonal cycle, and ENSO variability were found to be equivalent within error to modern coral records, but the errors are amplified due to the lengths of the records. However, combining multiple short pieces improves the skill of the final result, even when these pieces do not necessarily overlap in time. Most fossil coral records are not more than a few decades in length, so this work quantifies the uncertainty associated with limited record length.

The empirical event selection techniques and uncertainty quantification methodologies developed as part of this dissertation are powerful tools to be used in future multiproxy reconstructions. Although this work focuses on coral proxies, the same

methodologies could be applied to any proxy with at least annual resolution, providing a quantitative way to integrate disparate coral, tree ring, ice core, and varved sediment datasets. In particular, the event skill calculations provide a technique to weight records from varying parts of the Pacific, with low weight and high uncertainty assigned to records with low skill. A Monte Carlo simulation could be constructed to determine how many high- or low-skill records would be required to have confidence in an estimate of ENSO variability for a given time period, preventing erroneous assumptions about ENSO activity in pre-instrumental time periods that are due to limited datasets.

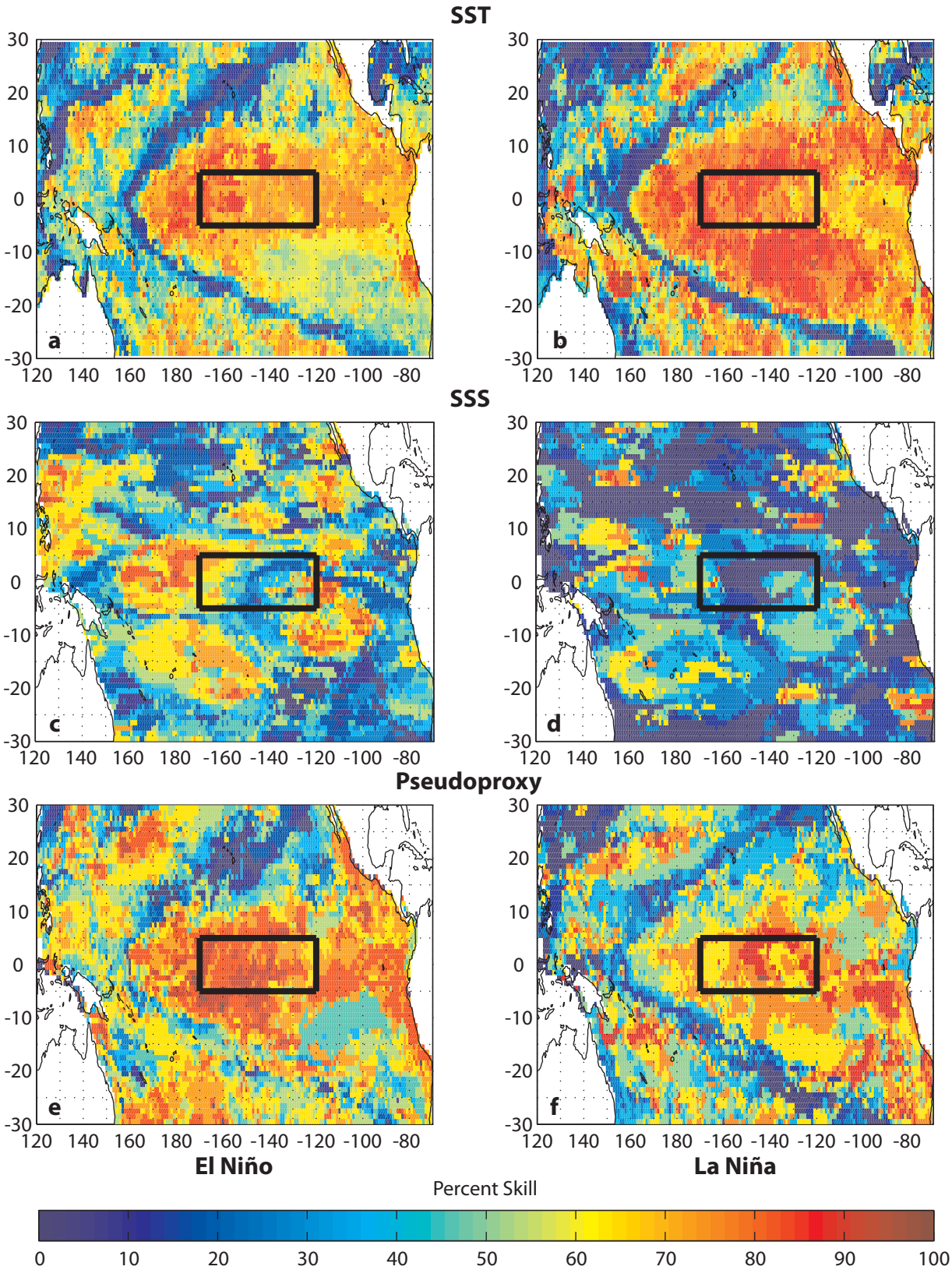

Figure 1.1. El Niño (left column) and La Niña (right column) skill percentages for (a, b) SST (1870-2010) (Rayner et al., 2003), (c, d) SSS (1970-2008) (Delcroix et al., 2011), and (e, f) the calculated pseudoproxy (1970-2008). The SST skill peak is located in the central and eastern Pacific, but the SSS skill peak is shifted west of the Niño 3.4 index region. The pseudoproxy data is calculated using a forward model (Thompson et al., 2011) of instrumental SST (Rayner et al., 2003) and SSS (Delcroix et al., 2011) to simulate coral $\delta^{18}O$. This data shows the net impact of constructive and destructive interference of SST and SSS as it would be recorded by corals.

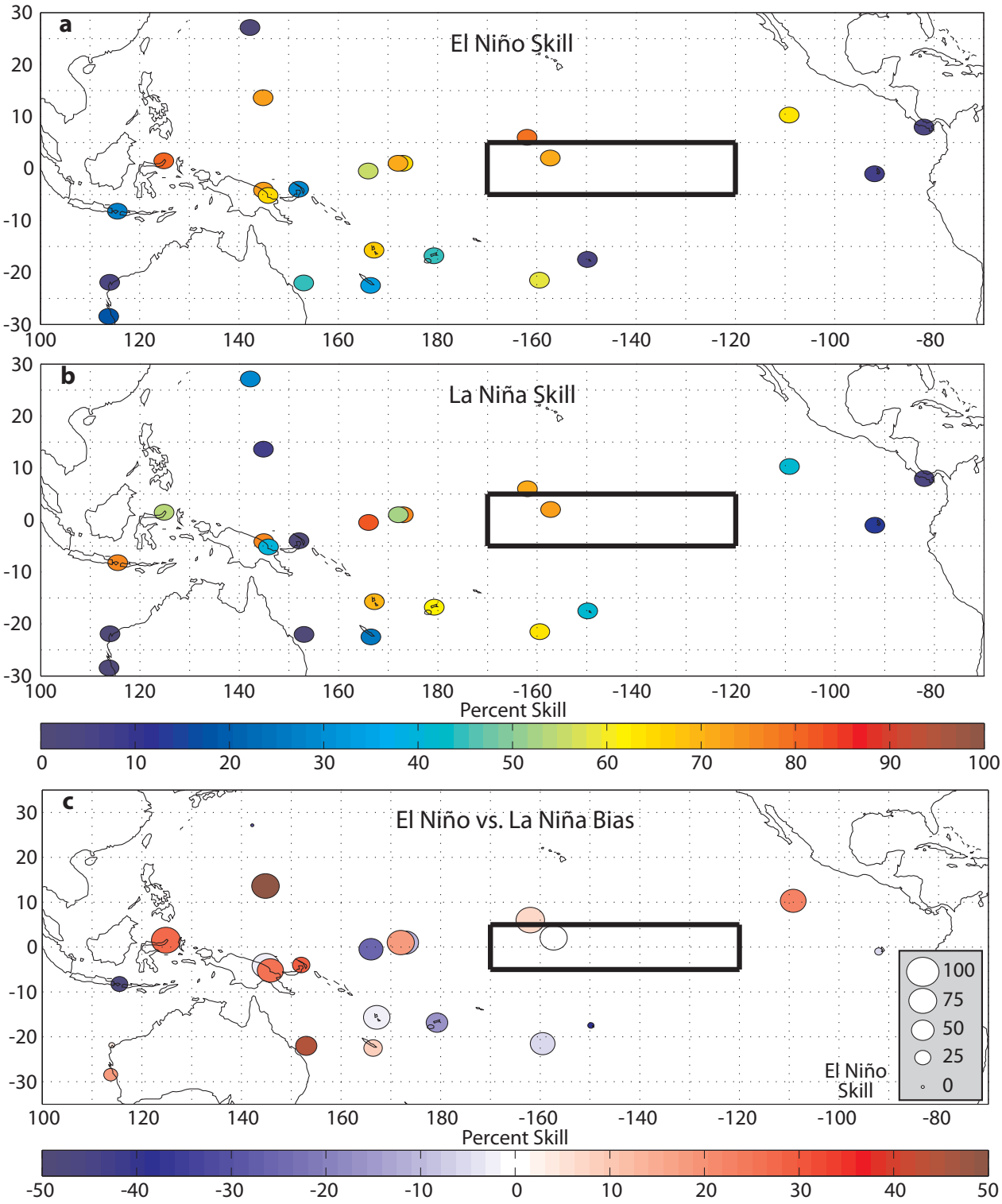

Figure 1.2. Map shows spatial distribution of (a) El Niño and (b) La Niña coral skill rates. Each dot corresponds to the location of a coral proxy record. The most accurate El Niño records are in the central and western Pacific. The most accurate La Niña records are in the central Pacific and SPCZ. Panel (c) shows the difference in skill between El Niño and La Niña event capture in coral records. Proxies in red record El Niño events with higher skill, and proxies in blue record La Niña events with higher skill. Stronger coloration indicates a larger bias in ENSO event capture. Circle size indicates El Niño skill for each location. El Niño events are preferentially recorded in the WPWP, La Niña events are most skillfully recorded in the SPCZ, and central Pacific records are balanced between El Niño and La Niña events.

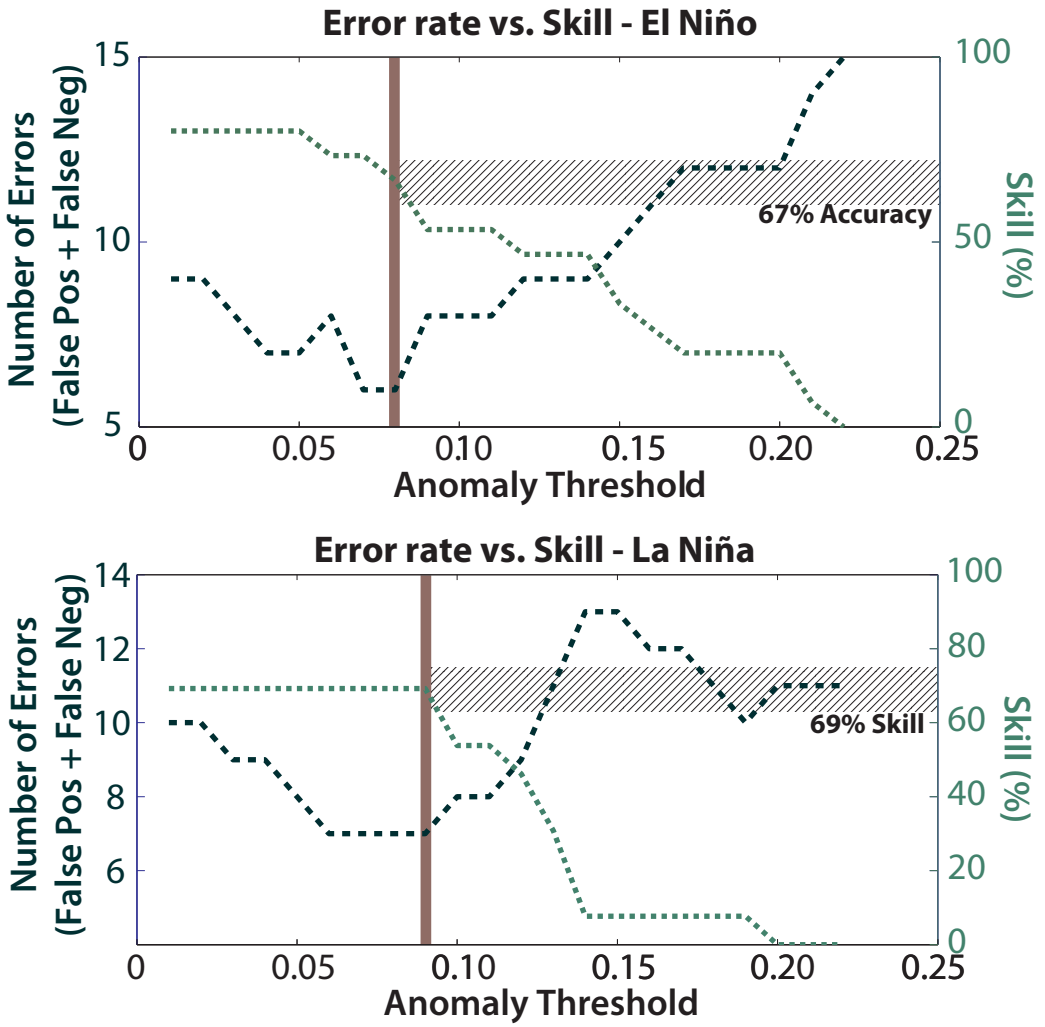

Figure 1.S1. Example of how ENSO threshold levels are calculated from Malo Channel, Vanuatu. Threshold level is selected to minimize errors (false positive + false negative events), and El Niño and La Niña threshold levels are calculated independently. Skill (% of correctly identified events in the instrumental record) declines as the threshold increases.

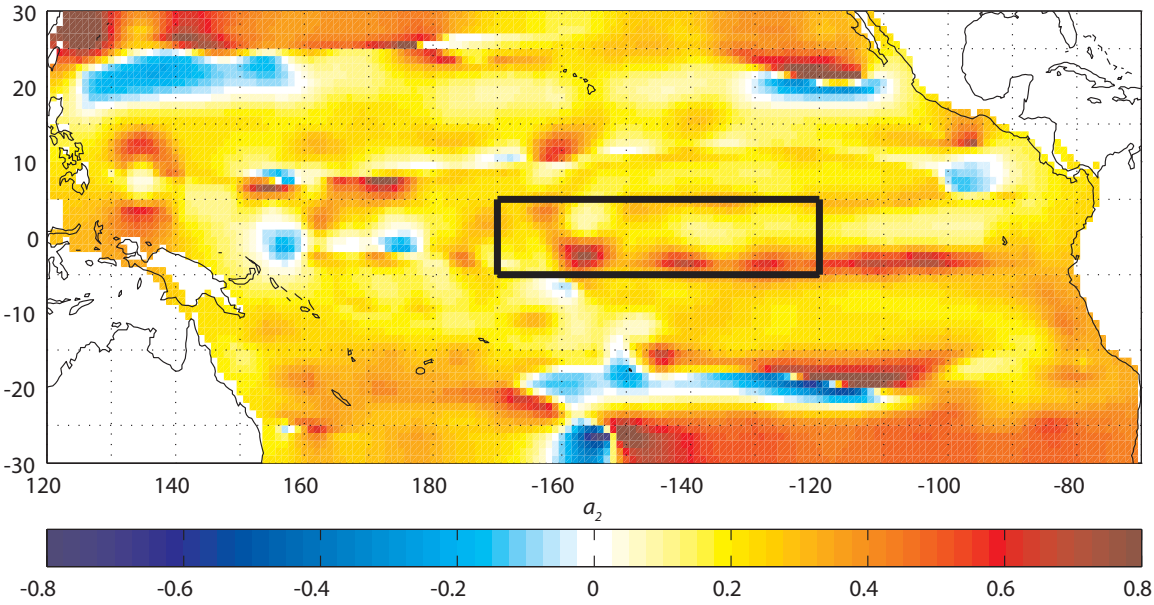

Figure 1.S2. Calculated SSS coefficients (a_2) show a wide range in variability due to local hydrology and water mass advection. Each grid cell was calculated by regressing mean SSS (Delcroix et al., 2011) against measured $\delta^{18}O$ (LeGrande and Schmidt, 2006) in a 3° x 3° region centered on the 1° x 1° grid cell.

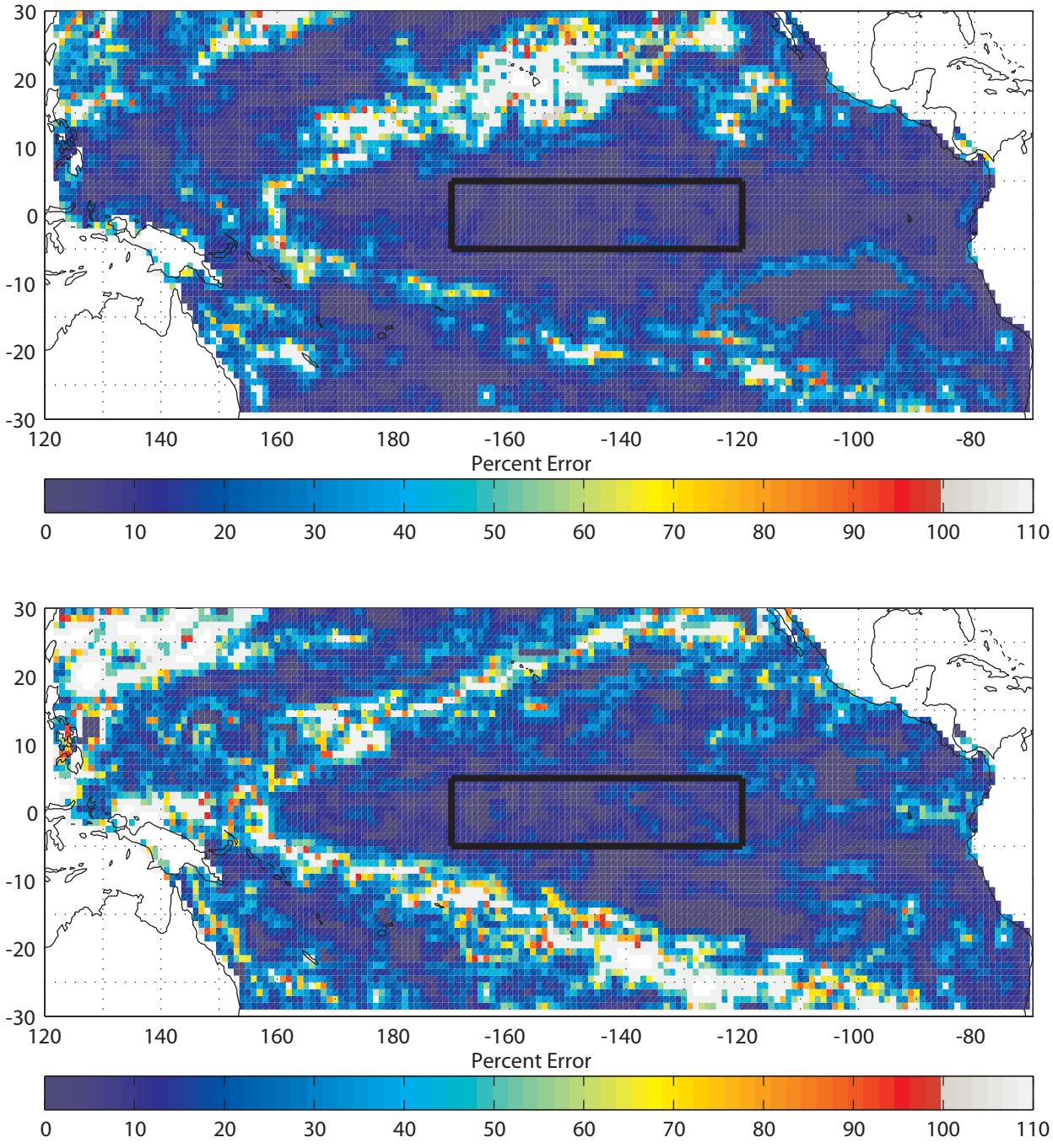

Figure 1.S3. El Niño (top) and La Niña (bottom) skill error as percentage of total skill for pseudoproxy data. Areas that exceed 100% are grayed out and should not be interpreted, as the error level exceeds the skill level in that region.

Table 1.S1. Summary of coral records included in analysis

Location	Author	Lat	Lon	Start Year	End Year
Guam	*Asami et al.* , 2005	13.6	144.8	1790	2000
Moorea	*Boiseau et al.* , 1998	-17.5	-149.8	1852	1989
Bunaken	*Charles et al.* , 2003	1.5	124.8	1863	1990
Lombok	*Charles et al.* , 2003	-8.3	115.5	1783	1990
Palmyra	*Cobb et al.* , 2003	6.0	-162.0	1886	1998
Abraham Reef	*Druffel and Griffin* , 1999	-22.0	153.0	1635	1989
Galápagos	*Dunbar et al.* , 1994	-1.0	-92.0	1607	1953
Kiritimati	*Evans et al.* , 1998	2.0	-157.3	1938	1993
Ogasawara	*Felis et al.* , 2009	27.1	142.2	1873	2002
Nauru	*Guilderson and Schrag* , 1999	-0.5	166.0	1895	1995
Vanuatu	*Kilbourne et al., 2004*	-15.7	167.2	1927	1992
Houtman Abrolhos	*Kuhnert et al.* , 1999	-28.5	113.8	1795	1993
Ningaloo	*Kuhnert et al.* , 2000	-21.9	114.0	1878	1994
Secas	*Linsley et al.* , 1994	8.0	-82.1	1707	1984
Clipperton	*Linsley et al.* , 2000	10.3	-109.2	1893	1994
Rarotonga	*Linsley et al.* , 2006	-21.5	-159.5	1726	2000
New Caledonia	*Quinn et al.* , 1998	-22.5	166.5	1658	1993
Rabaul	*Quinn et al.* , 2006	-4.0	152.0	1867	1997
Laing	*Tudhope et al.* , 2001	-5.2	145.8	1880	1993
Madang	*Tudhope et al.* , 2001	-4.2	144.9	1884	1993
Maiana	*Urban et al.* , 2000	1.0	173.0	1840	1995
Fiji	*Bagnato et al.* , 2005	-16.8	179.2	1776	2001
Tarawa	*Cole et al.* , 1993	1.0	172.0	1894	1990

Table 1.S2. Accuracy, errors, and thresholds for coral records

Location	El Niño skill (%)	La Niña skill (%)	# Correct (Niño)	# Correct (Niña)	False pos (Niño)	False neg (Niño)	False pos (Niña)	False neg (Niña)	El Niño threshold	La Niña threshold
Guam	72	8	21	2	7	8	1	24	0.02	0.10
Moorea	4	42	1	10	0	25	4	14	0.20	0.10
Bunaken	81	54	21	13	6	5	2	11	0.06	0.14
Lombok	27	75	7	18	3	19	11	6	0.16	0.07
Palmyra	79	71	22	15	3	6	5	6	0.08	0.09
Abraham Reef	44	0	11	0	9	14	0	21	0.06	0.23
Galápagos	6	13	1	2	0	15	0	14	0.27	0.23
Kiritimati	71	73	10	8	0	4	1	3	0.10	0.14
Ogasawara	0	29	0	7	0	28	2	17	0.19	0.10
Nauru	56	82	14	14	4	11	7	3	0.17	0.11
Vanuatu	67	69	10	9	1	5	5	4	0.08	0.09
Houtman Abrolhos	19	0	5	0	4	22	0	24	0.11	0.26
Ningaloo	4	0	1	0	0	26	0	20	0.19	0.20
Secas	4	4	1	1	0	24	0	22	0.35	0.28
Clipperton	64	41	16	7	3	9	0	10	0.04	0.09
Rarotonga	59	64	17	16	10	12	6	9	0.05	0.06
New Caledonia	33	25	9	6	5	18	3	18	0.11	0.12
Rabaul	30	0	8	0	2	19	0	24	0.13	0.32
Laing	73	75	19	15	1	7	13	5	0.08	0.03
Madang	65	40	17	8	7	9	6	12	0.07	0.13
Maiana	64	75	18	18	0	10	8	6	0.13	0.09
Fiji	45	62	13	16	3	16	11	10	0.09	0.03
Tarawa	71	53	17	9	4	7	1	8	0.08	0.14

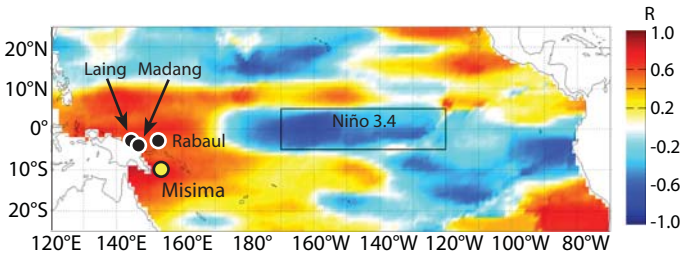

Figure 2.1. Study Location. Correlation map (R) showing the relationship between Niño 3.4 SST anomalies and Pacific SSS anomalies (Delcroix et al., 2011) in December of known El Niño event years, when central Pacific SST anomalies are largest. Yellow circle denotes location of Misima, and black circles indicate other modern coral records used in this study. Niño 3.4 region, black box, is a standard El Niño-Southern Oscillation (ENSO) index region. Strong positive correlation in the WPWP (R = 0.78 at Misima) indicates increases in salinity as the central Pacific warms.

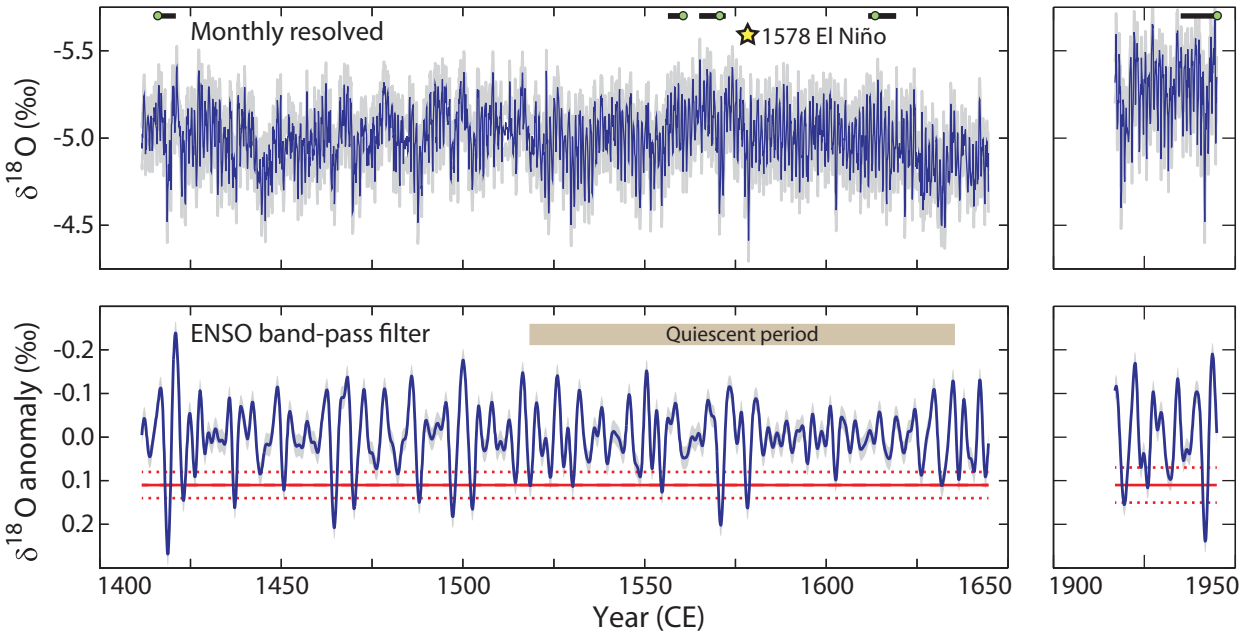

Figure 2.2. Coral-based El Niño reconstruction at Misima. Monthly resolved and band-pass filtered Misima $\delta^{18}O$ records for fossil (left) and modern (right) corals. Age model is constructed using ^{230}Th dates (green circles) that have been shifted within error (black lines) to align with the known 1578 historical El Niño event (yellow star). Sections of filtered record that fall below the empirical El Niño event threshold, red line ($\pm 1\sigma$, red dotted line), correspond to El Niño events. Error range, gray cloud, reflects replication error (1σ). ENSO quiescence begins in early 1500's and extends through early 1600's.

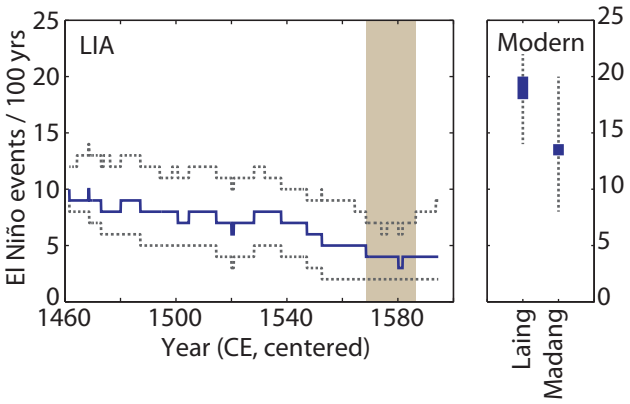

Figure 2.3. El Niño event reconstruction. 100-year running count of El Niño events (defined by empirical isotopic event threshold, 0.11 ± 0.03‰), in Little Ice Age (LIA) Misima record, blue line (year given is window center), compared with running 100-year segments of modern coral records, blue rectangles (Tudhope et al., 2001). Although the earliest part of the Misima record is comparable to modern records in events/century, number of events/century declines precipitously into the 1500's. The period 1519–1636 CE (centered on brown bar) has fewer events per century than any time in the modern PNG records.

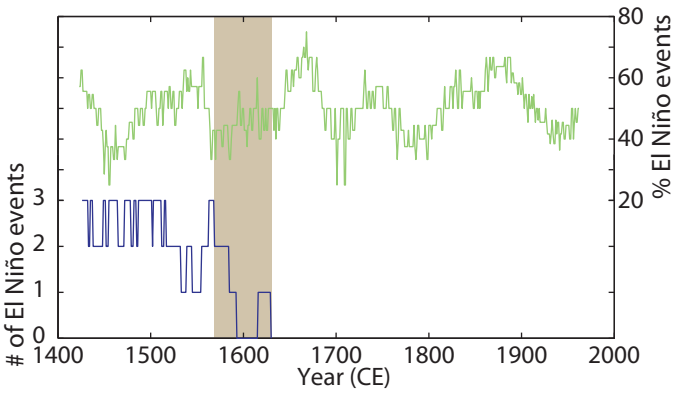

Figure 2.4. Relative contributions of El Niño to La Niña events to ENSO signal. El Niño to La Niña event rates over 30-year running windows in a tree ring reconstruction of Niño 3, top (D'Arrigo et al., 2005). 30-year running count of El Niño events at Misima, bottom, declines over a relative minimum in the contribution of El Niño events to the total ENSO signal (brown bar). The decline in El Niño events at Misima therefore may be driven by either a decline in total ENSO variability or an increased proportion of La Niña events.

Near-modern (MiC)

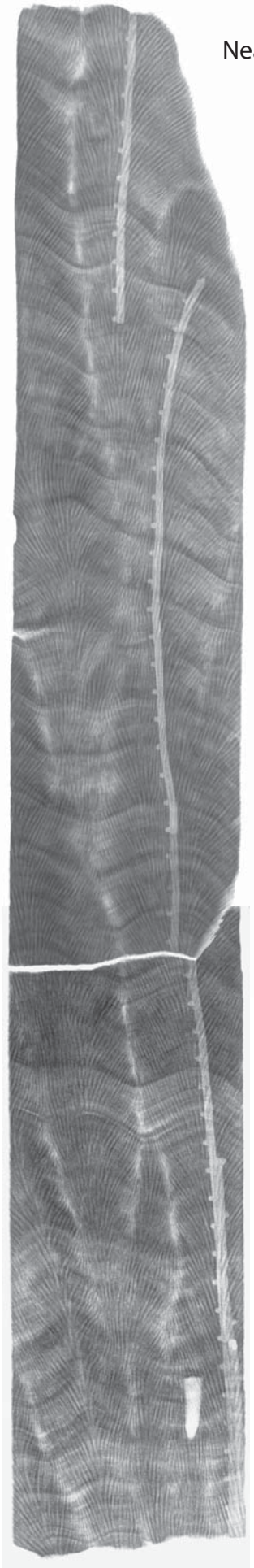

Fossil (MiF)

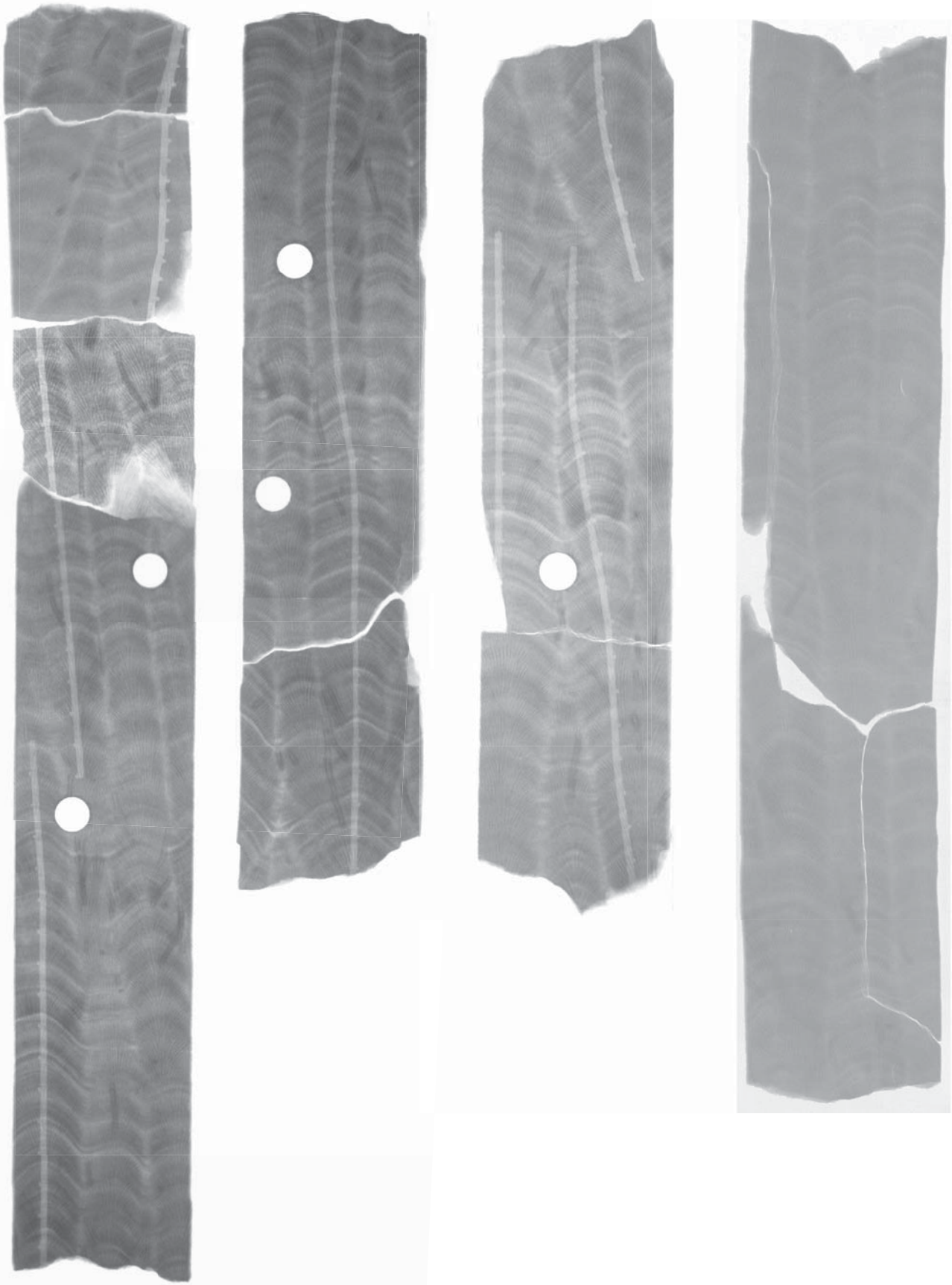

Fossil (MiG)

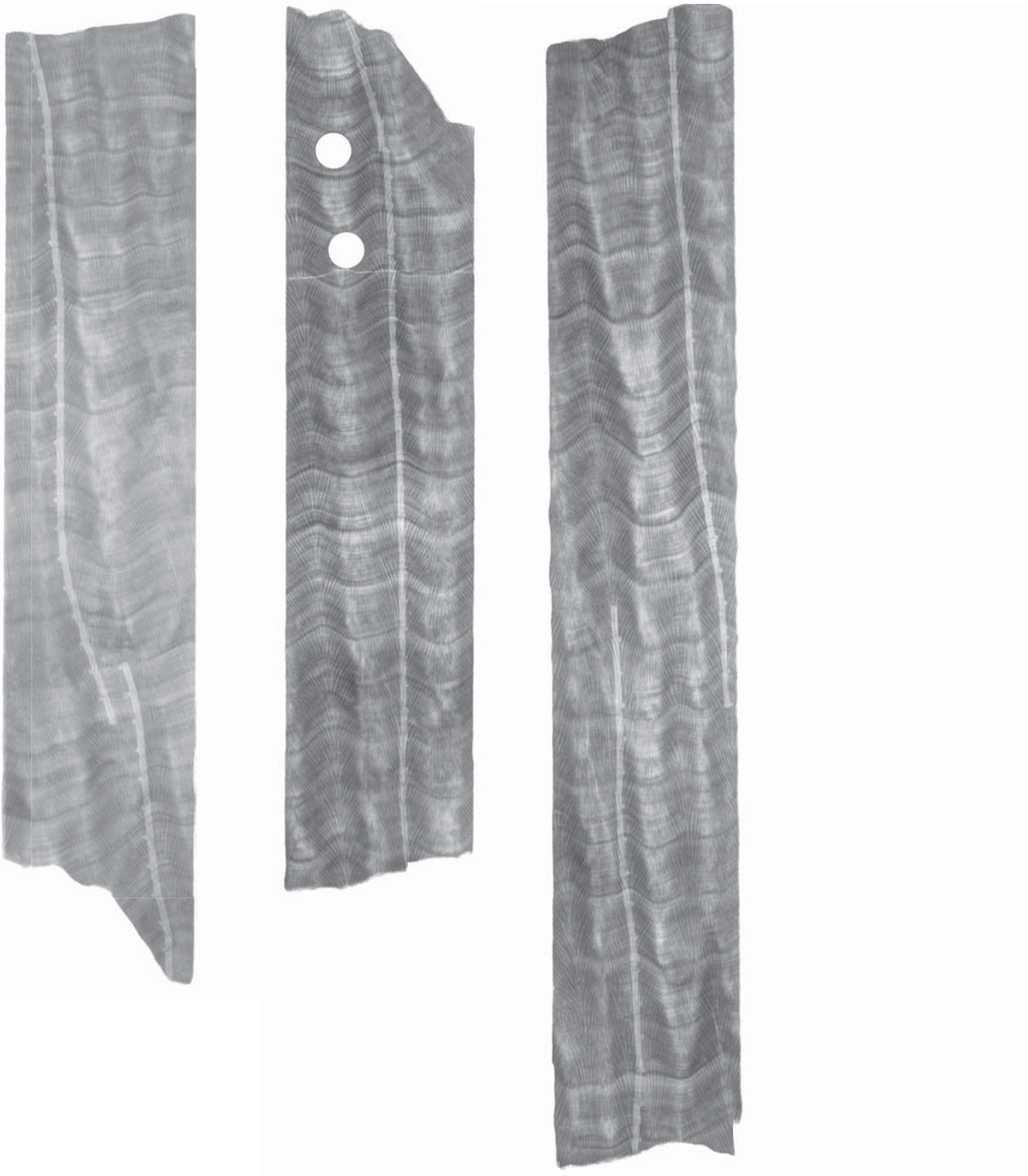

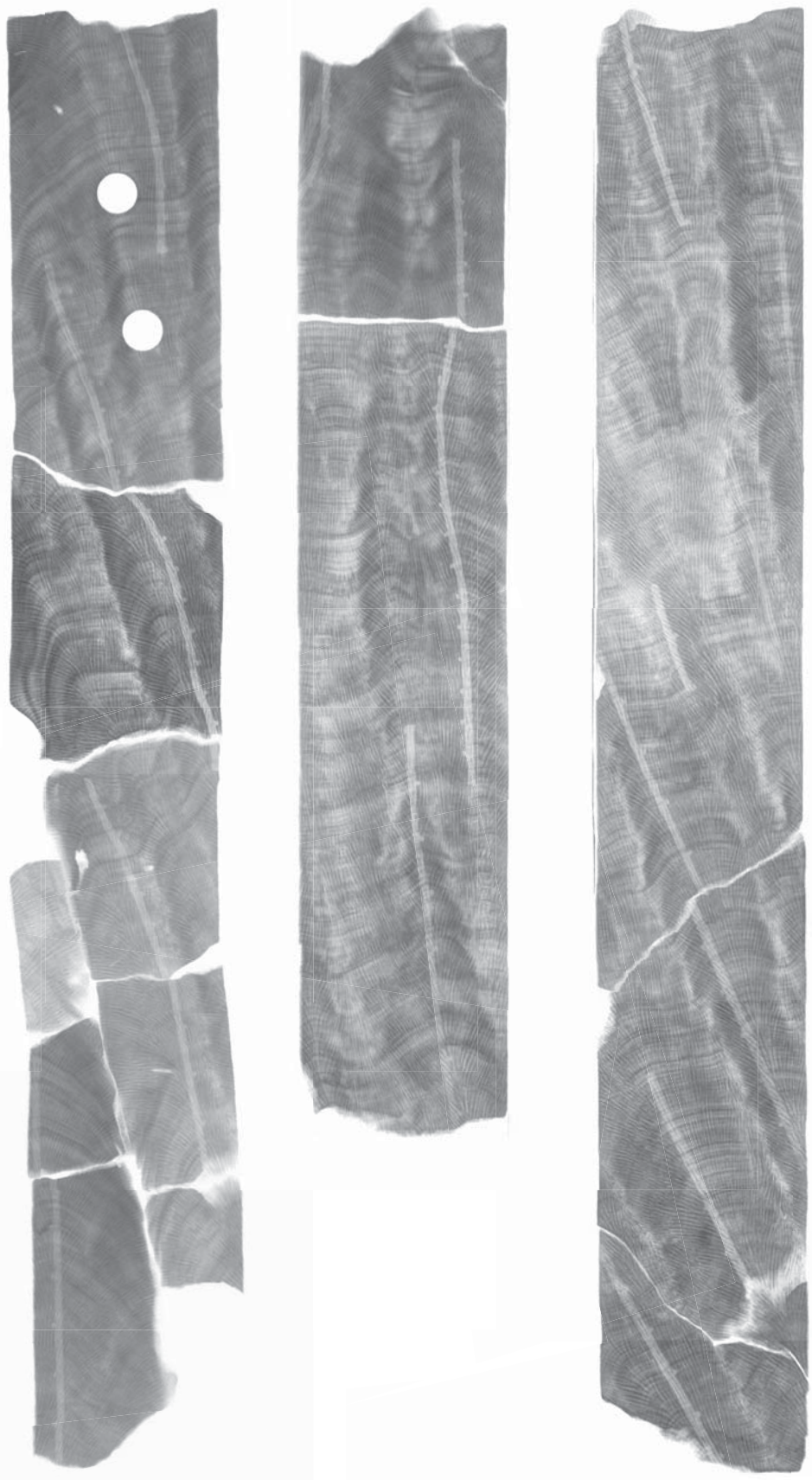

Figure 2.S1. X-ray images. X-ray images of modern and fossil Misima corals show drilling paths along growth axes.

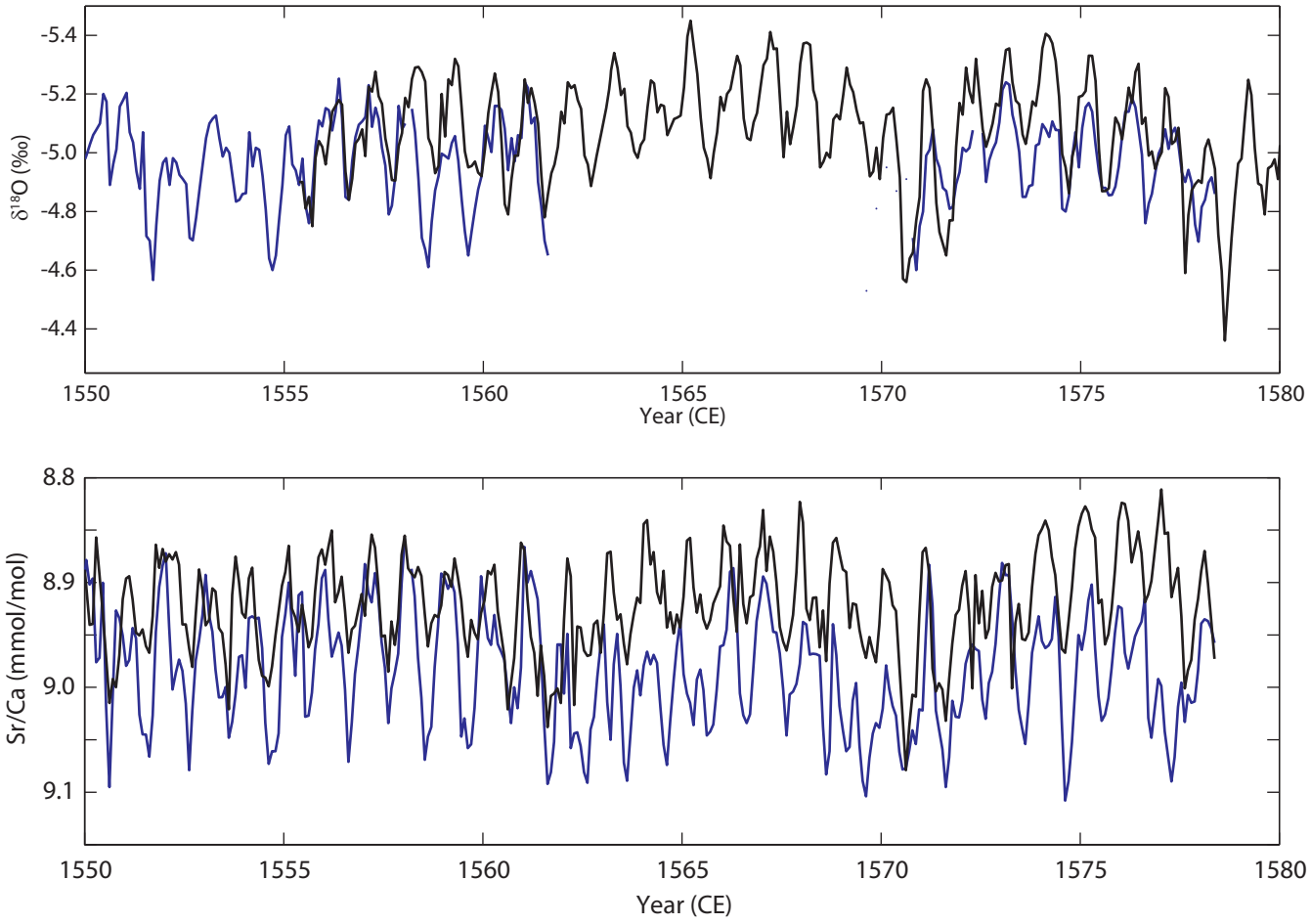

Figure 2.S2. Core overlaps. Overlaps between cores showing reproduced sections for $\delta^{18}O$ and Sr/Ca. No mean adjustments have been applied. The oxygen isotope record shows the excellent reproducibility of this record. The Sr/Ca data is more variable, but the long-term means of both datasets are equivalent.

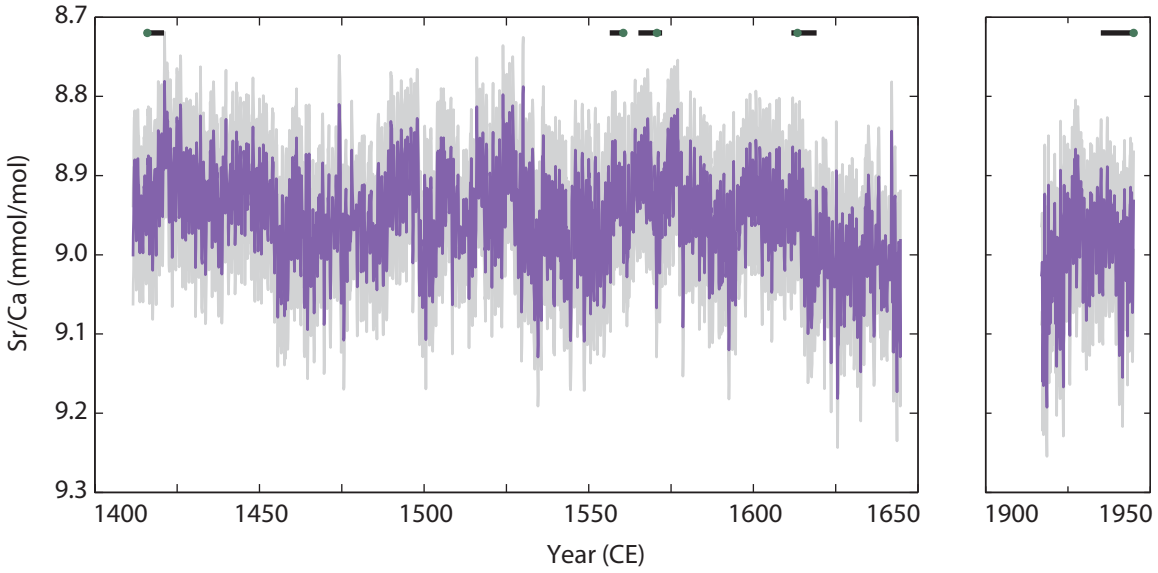

Figure 2.S3. Monthly resolved Misima Sr/Ca data. Despite the range in Sr/Ca variability, there is no significant mean change between the fossil and modern records (error = ±0.062 mmol/mol, 1σ, gray cloud). Combined with the significant mean change in the $\delta^{18}O$ record, this suggests that the LIA was drier, but not necessarily cooler, than the modern climate in the region.

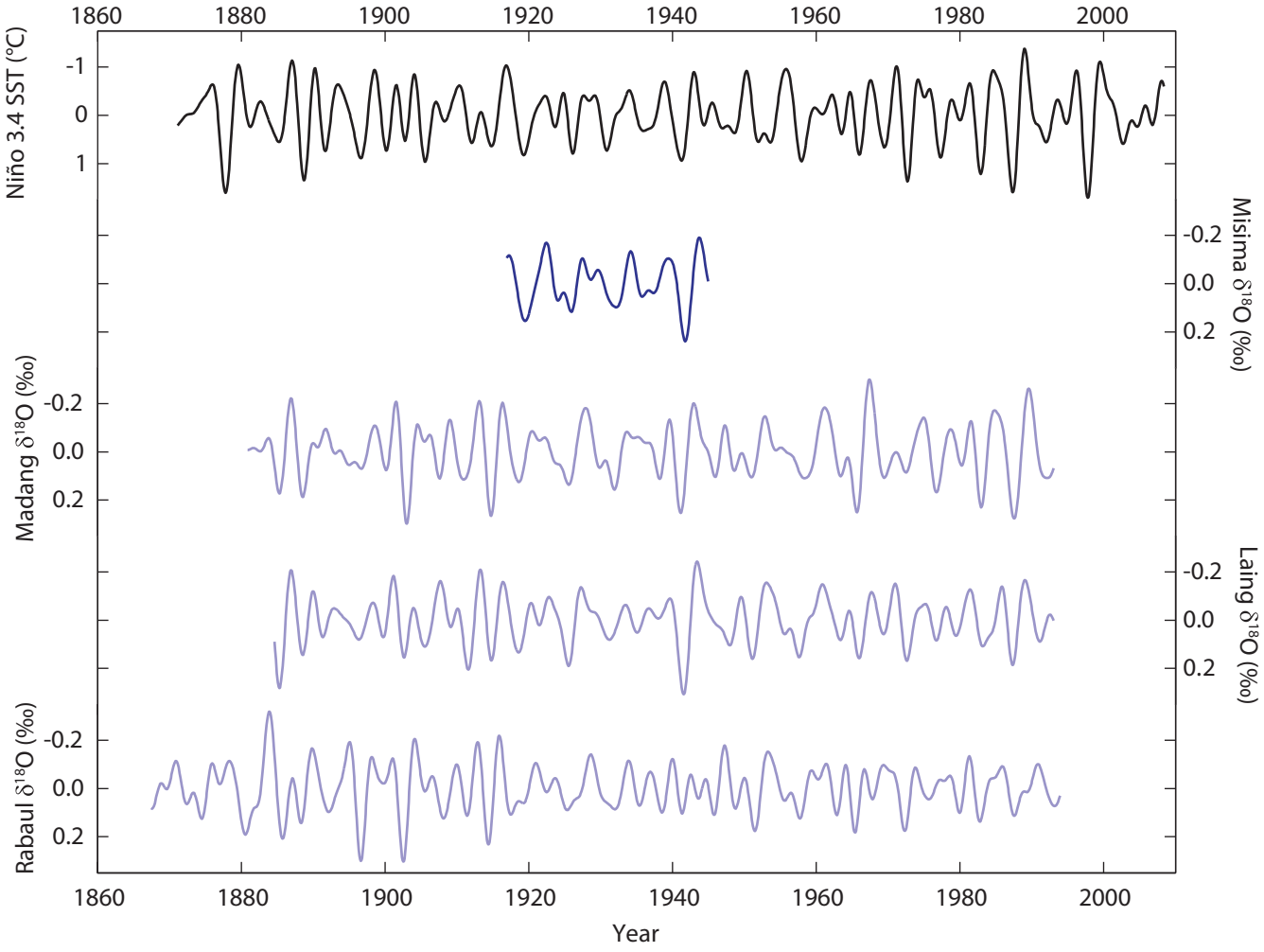

Figure 2.S4. ENSO signal in modern PNG corals. The Niño 3.4 instrumental record of ENSO variability compared with modern band-pass filtered sub-annually resolved coral $\delta^{18}O$ records at Misima, Madang, Laing, and Rabaul (Quinn et al., 2006; Tudhope et al., 2001) show that PNG corals are robust recorders of ENSO activity. The strong 1941/42 El Niño event and comparable decadal-scale variability suggest that these records can be compiled to calibrate the fossil Misima coral with modern conditions.

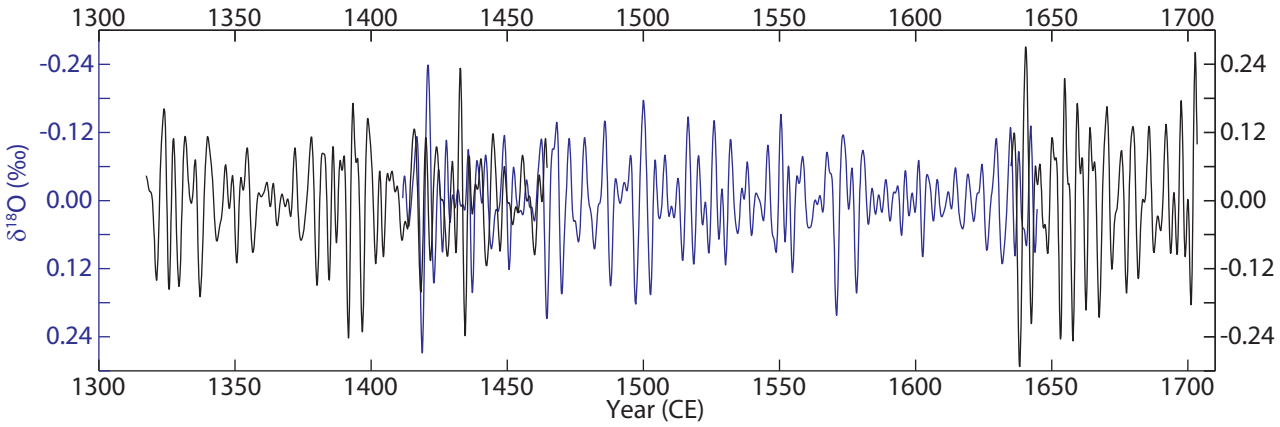

Figure 2.S5. Misima (blue) and Palmyra (black, Cobb et al., 2003) coral records showing overlapping time intervals. Due to age uncertainties in each record and differing sensitivities to El Niño and La Niña events, it is difficult to isolate matching ENSO events; however, both records show a similar magnitude in El Niño response. Note that axes are reversed to reflect opposing regional SSS/SST responses to ENSO events.

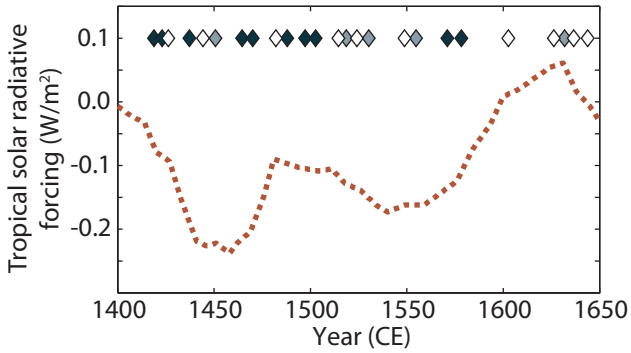

Figure 2.S6. Solar activity as a predictor for El Niño event frequency. Solar activity (Mann et al., 2005) (orange dashed line) versus El Niño events at Misima (diamonds). Dark blue diamonds are most likely El Niño events, light blue are probable events, and white are possible events. Although some events appear to cluster at relative solar maxima, absolute solar radiation does not correlate well with El Niño event timing. This suggests that there is not a linear relationship between ENSO and solar activity on multidecadal time scales.

$\delta^{234}U$ measured	^{230}Th / ^{238}U (activity)	^{230}Th / ^{232}Th ppm	Age (yr) uncorrected	Age (yr) corrected	$\delta^{234}U_{Initial}$ corrected	**Year CE**	Lab
148.4 ±2.1	0.0008 ±0.000013	36 ±0.8	75 ±1	66 ±5	148 ±2	**1940 ±5**	University of
147.8 ±1.6	0.0062 ±0.000029	2187 ±143.6	589 ±3	588 ±3	148 ±2	**1418 ±3**	Minnesota

$\delta^{234}U$ measured	$^{230}Th/^{238}U$ activity	$^{230}Th/^{232}Th$ ppm	Age (yr) uncorrected	Age (yr) corrected	$\delta^{234}U_{initial}$ corrected	**Year CE**	Lab
149.2 ± 3.1	0.0047 ± 0.000025	4483 ± 214	452.1 ± 2.7	451.7 ± 2.7	149.4 ± 3.1		National Taiwan
150.8 ± 3.5	0.0047 ± 0.000032	5345 ± 508	450.9 ± 3.4	450.6 ± 3.4	151.0 ± 3.5		University
			wt-averaged date	*451.3 ± 2.1*		**1559 ± 2**	

$\delta^{234}U$ measured	$^{230}Th/^{238}U$ activity	$^{230}Th/^{232}Th$ ppm	Age (yr) uncorrected	Age (yr) corrected	$\delta^{234}U_{initial}$ corrected	**Year CE**	Lab
146.3 ± 0.8	0.0046 ± 0.000032	3656 ± 118	442.5 ± 3.1	440.6 ± 3.6	146.4 ± 0.8	**1569 ± 4**	University of
145.1 ± 0.7	0.0041 ± 0.000033	2813 ± 76	396.0 ± 3.2	393.9 ± 3.8	145.2 ± 0.7	**1615 ± 4**	Texas

Table 2.S1. ^{230}Th dating information. List of timing and error on dates used to constrain coral chronology. Sections of coral core were shifted within noted error ranges to match a known historical ENSO event. Samples were dated using a Finnegan MAT Element inductively coupled plasma mass spectrometer at the University of Minnesota Isotope Laboratory, a Thermo Neptune multicollector inductively coupled plasma mass spectrometer at the National Taiwan University, and a Thermo Scientific Triton thermal ionizaiton mass spectrometer at the University of Texas at Austin.

Location of Coral studies	Location	Growth Interval (CE)	Length (years)
Misima Fossil	10.6°S, 152.8°E	1411-1644	233
Misima Modern	10.6°S, 152.8°E	1915-1944	28
Madang (Tudhope et al., 2001)	5.2°S, 145.8°E	1880-1993	113
Laing (Tudhope et al., 2001)	4.2°S, 144.9°E	1884-1993	109
Rabaul (Quinn et al., 2006)	4°S, 152°E	1867-1997	130

Table 2.S2. Study location. Location and growth information for *Porites* coral records in study. Fossil record is compared with a modern record from Misima and published modern centennial-scale records from PNG.

Misima Fossil	1411-1644 CE	**Misima**	1915-1944 CE	**Madang**	1880-1993 CE	**Laing**	1884-1993 CE	**Rabaul**	1867-1997 CE
Year	*δ^{18}O Anom (‰)*	*Year*	*δ^{18}O Anom (‰)*	*Year*	*δ^{18}O Anom (‰)*	*Year*	*δ^{18}O Anom (‰)*	*Year*	*δ^{18}O Anom (‰)*
1418.792	0.27							1880.542	0.19
1423.042	0.15			1885.292	0.17	1885.292	0.28	1885.792	0.21
1437.208	0.16			1888.542	0.19	1888.542	0.14		
1450.708	0.12					1896.375	0.08	1896.625	0.3
1464.542	0.21			1903.042	0.30	1902.625	0.16	1902.542	0.3
1470.042	0.16					1905.542	0.11		
1487.958	0.15			1907.625	0.11				
1497.208	0.18			1910.958	0.12				
1502.625	0.17					1911.625	0.21		
1518.542	0.11			1914.792	0.27	1914.792	0.17	1914.375	0.23
1530.208	0.11	1919.542	0.16	1918.625	0.13	1918.542	0.13		
1554.792	0.13	1925.958	0.12	1925.542	0.14	1925.542	0.19		
1570.958	0.20					1931.208	0.08		
1578.292	0.16			1931.958	0.16				
1631.792	0.11			1938.208	0.11				
		1941.792	0.24	1941.125	0.25	1941.542	0.31		
						1947.958	0.10		
						1951.125	0.16	1951.458	0.18
						1957.625	0.15		
						1963.375	0.08		
				1965.708	0.25	1965.958	0.16	1965.375	0.18
						1972.625	0.17	1972.292	0.18
				1976.708	0.17	1976.708	0.08		
				1982.958	0.23	1983.208	0.11		
				1987.542	0.28	1987.375	0.19		
						1991.125	0.09		

Table 2.S3. Timing of El Niño events in PNG coral records. Listing of identified El Niño events for all PNG records used in this study, with the filtered coral δ^{18}O anomaly. Modern events are aligned if they fall within known instrumental El Niño events, ±4 months to account for standard coral age model uncertainty. Events that are correctly picked in the Misima record and other modern PNG records are highlighted in blue; events that are correctly picked only in other PNG records are highlighted in red. False positive events (that do not correspond with known El Niño events) are grayed out.
Event identification has a high degree of spatial coherence, which supports the notion of using the modern PNG records to calibrate the fossil record.

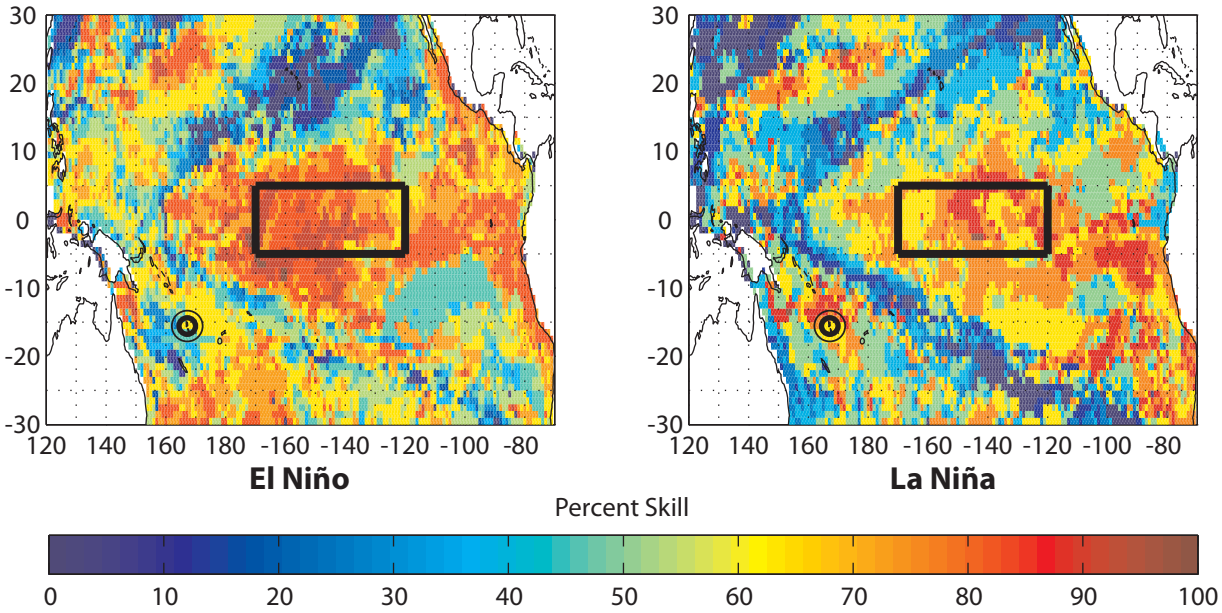

Figure 3.1. El Niño (left column) and La Niña (right column) skill percentages for calculated pseudoproxy (1970-2008). The pseudoproxy data is calculated using a forward model (Thompson et al., 2011) of instrumental SST (Rayner et al., 2003) and SSS (Delcroix et al., 2011) to simulate coral $\delta^{18}O$. Skill assessments are relative to the Niño 3.4 index region (box). Vanuatu (circle) coral data are expected to record approximately 60% of both El Niño and La Niña events based on the pseudoproxy analysis. (Modified from Hereid et al., in revision, 2012)

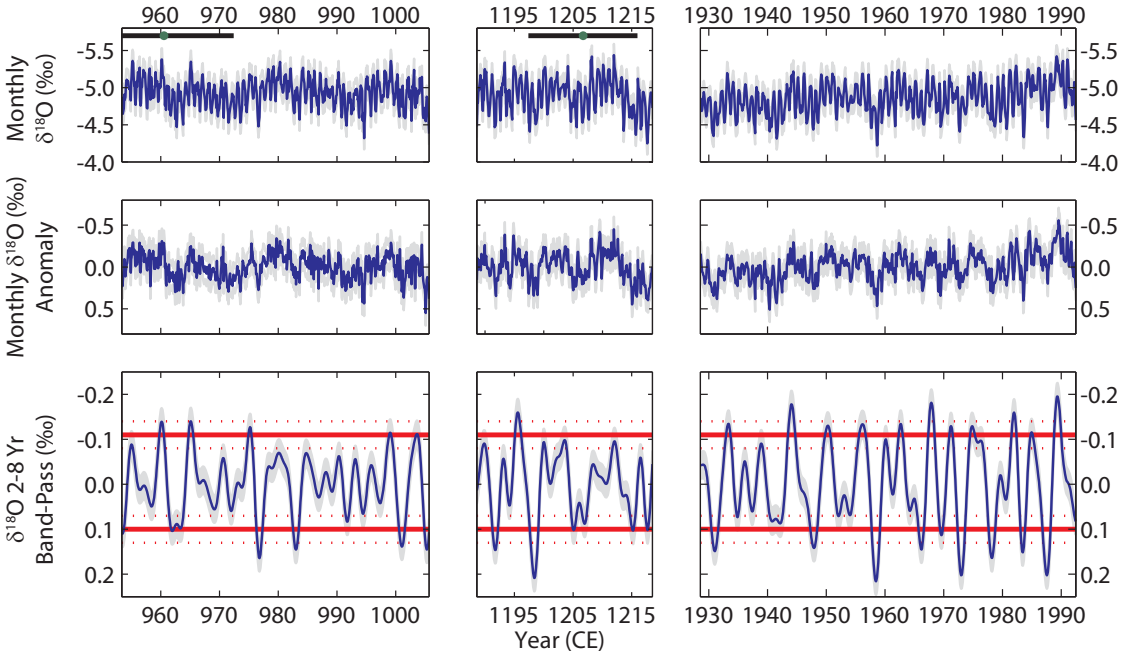

Figure 3.2. Monthly resolved, monthly anomaly, and band-pass filtered (2-8 year) data. Left two panels are fossil corals, right panel is Malo Channel, Vanuatu modern record (Kilbourne et al., 2004). Red lines are El Niño and La Niña thresholds (dotted lines reflect threshold error). Green circles are ^{230}Th dates, with associated error bars (black lines).

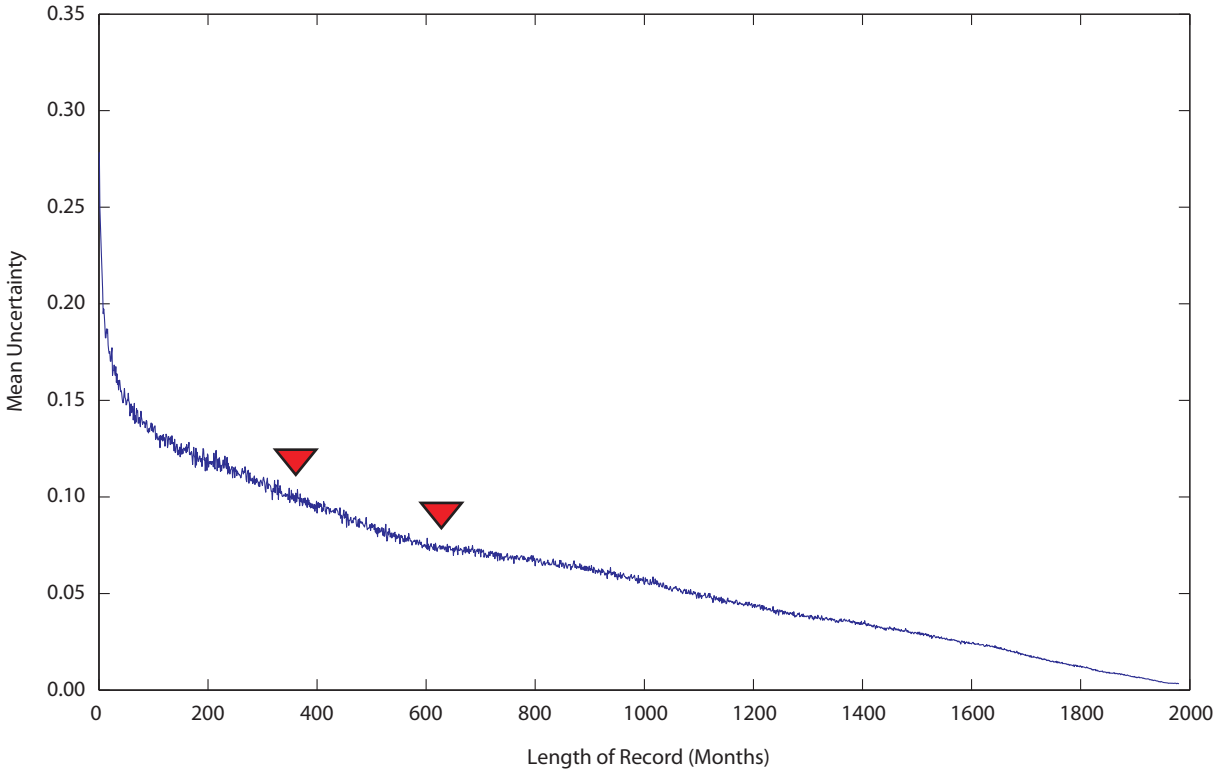

Figure 3.3. Uncertainty as a function of record length derived from 1000 iterations of a Monte Carlo simulation incorporating replication uncertainty on the modern 165 year SBV core. This analysis demonstrates the error in mean climate state due to selecting multidecadal sections within a longer time series. Red triangles indicate the lengths of the fossil records included in the study.

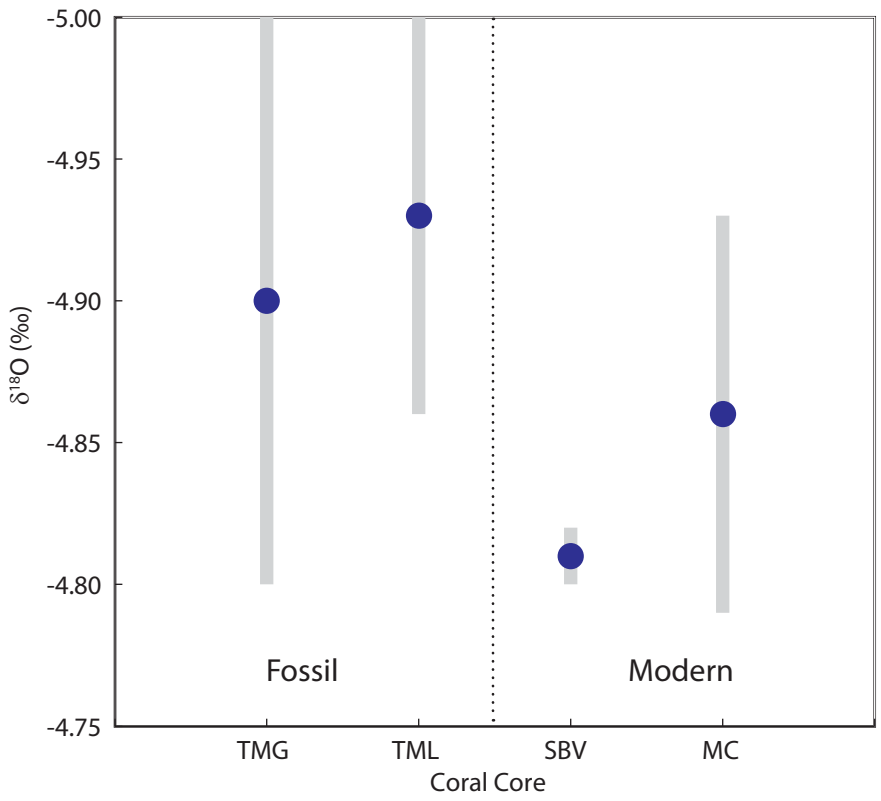

Figure 3.4. Estimates of mean values (blue dots) and uncertainty (gray bars, includes replication and record length uncertainty) for fossil cores TMG (31 years), TML (53 years), SBV (165 years), and MC (64 years). Since the SBV record was used to calibrate record length uncertainty, the error bar for that record only represents intercolony replication error. The means for the fossil and modern records generally are equivalent within uncertainty.

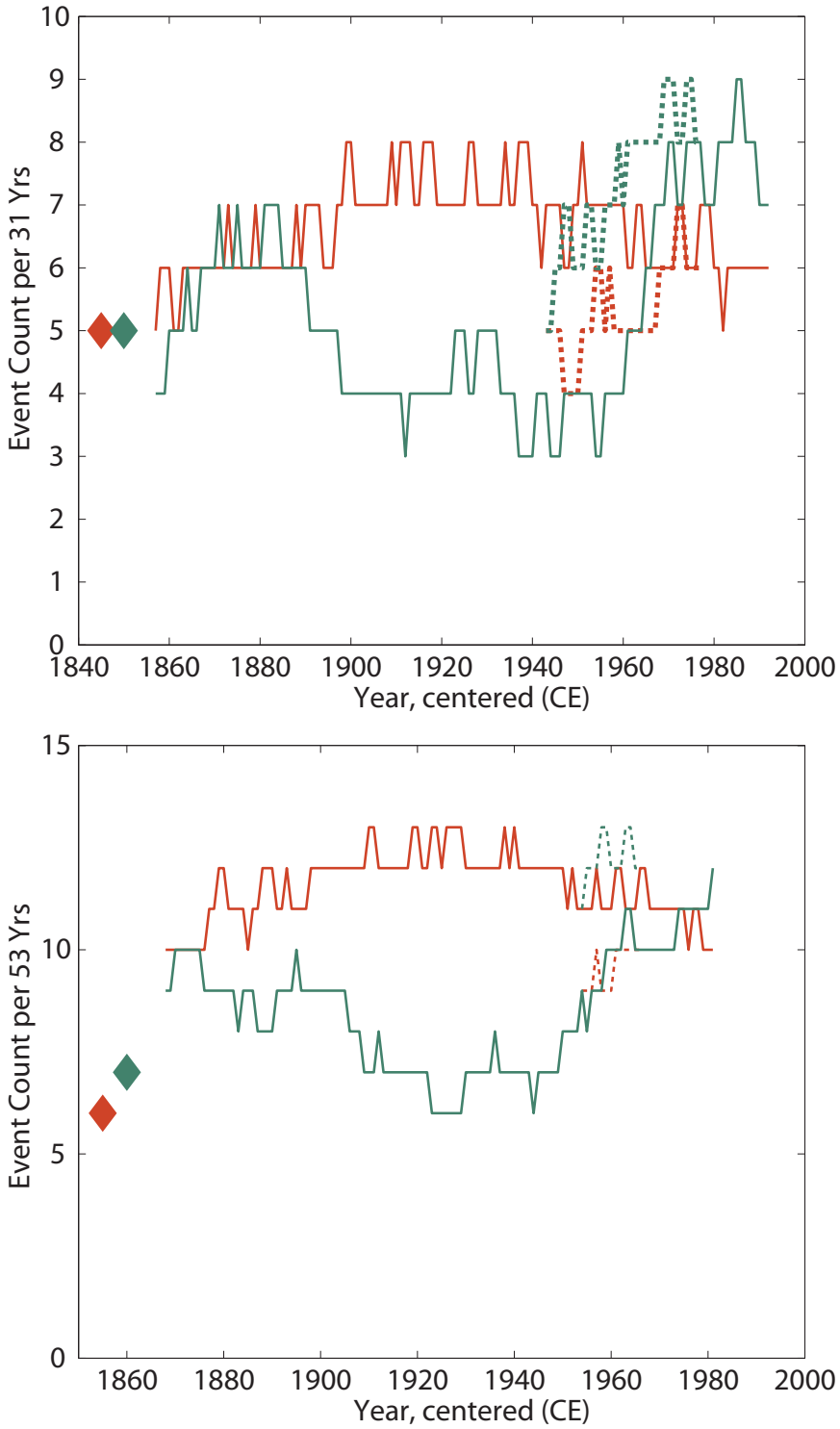

Figure 3.5. Running event counts of modern records (solid - SBV, dashed - Malo Channel) in 31 year window (top) and 53 year window (bottom) to match the lengths of the fossil records. Fossil record event counts shown with diamonds. Orange signifies El Niño event count, green is La Niña event count. Fossil event counts are generally lower than modern even counts, but overlap during periods of reduced ENSO activity in the mid-twentieth century.

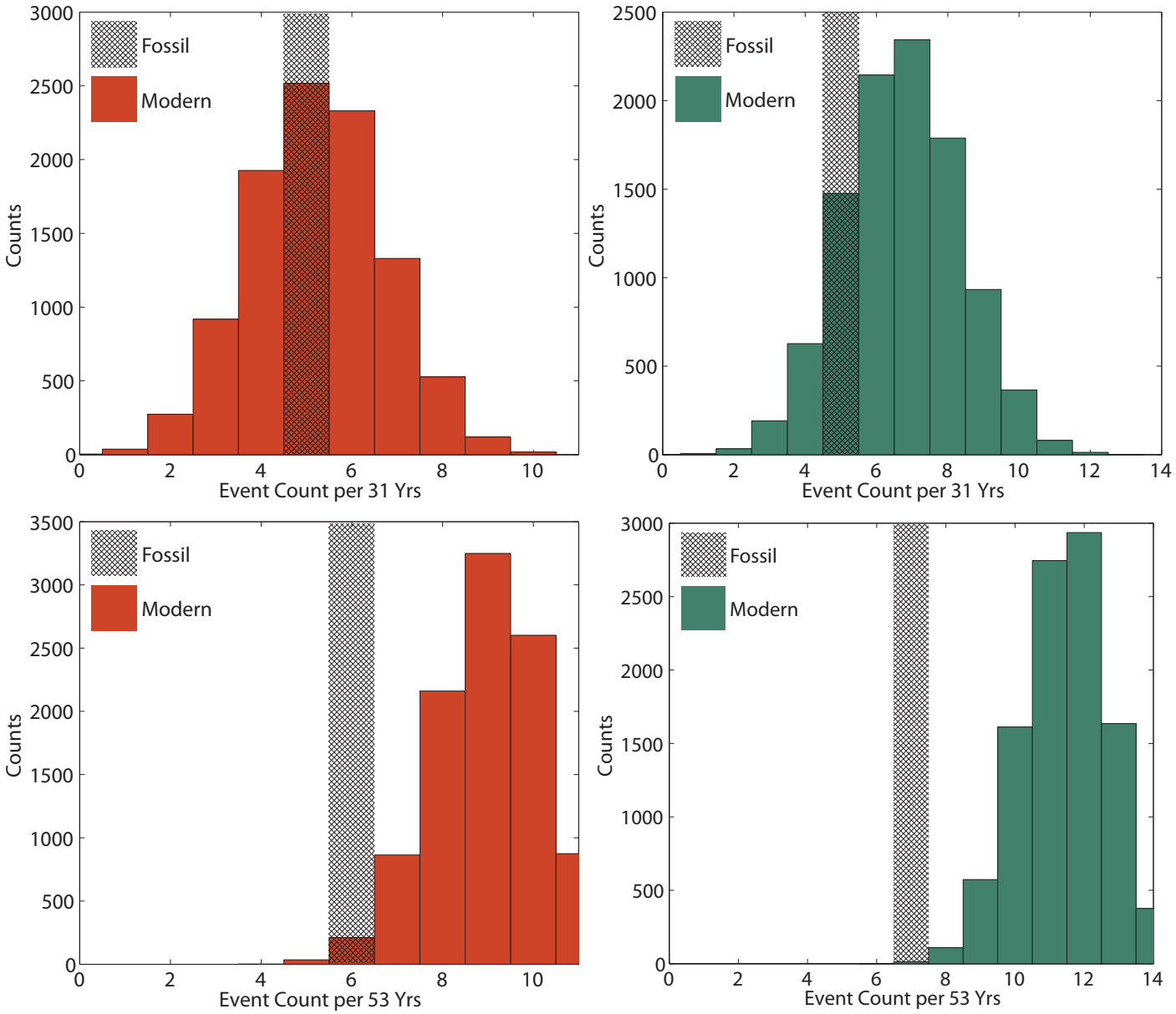

Figure 3.6. Bootstrap event count distribution comparison between the fossil and modern Malo Channel records shows the differences among El Niño (orange) and La Niña (green) event rates through time. Colored bars show potential random event distributions for 31 (top row) and 53 (bottom row) year periods in the modern record. Hatched bar shows actual fossil event counts. 53 year fossil record has significantly lower ENSO event rates than the modern Malo Channel record ($p < 0.05$), but 31 year record falls within the range of modern ENSO variability.

Author Contributions

Chapter 1: K.A.H developed the data analysis techniques, designed and implemented the software, and wrote the paper. T.M.Q. supervised the project and provided feedback on the manuscript. Y.M.O. provided feedback on the proxy skill analysis and manuscript.

Chapter 2: K.A.H. conducted the coral geochemical analyses and statistical analyses, developed the data analysis techniques, provided ^{230}Th dates, and wrote the paper. T.M.Q. acquired funding, supervised the project, and provided feedback on the manuscript. F.W.T. acquired funding and collected the coral samples. R.L.E. acquired funding and provided ^{230}Th dates. H.C. provided ^{230}Th dates. C.-C. S. provided ^{230}Th dates and provided feedback on the manuscript.

Chapter 3: K.A.H. conducted the coral geochemical analyses and statistical analyses, developed the data analysis techniques, and wrote the paper. T.M.Q. acquired funding, supervised the project, and provided feedback on the manuscript. F.W.T. acquired funding and collected the coral samples. R.L.E. acquired funding and provided ^{230}Th dates. H.C. and C.-C. S. provided ^{230}Th dates.

References

Asami, R., Yamada, T., Iryu, Y., Quinn, T. M., Meyer, C. P., and Paulay, G., 2005, Interannual and decadal variability of the western Pacific sea surface condition for the years 1787-2000: Reconstruction based on stable isotope record from a Guam coral: Journal of Geophysical Research-Oceans, v. 110, no. C5.

Ashok, K., Behera, S. K., Rao, S. A., Weng, H. Y., and Yamagata, T., 2007, El Nino Modoki and its possible teleconnection: Journal of Geophysical Research-Oceans, v. 112, no. C11, p. 27.

Bagnato, S., Linsley, B. K., Howe, S. S., and Wellington, G. M., 2005, Coral oxygen isotope records of interdecadal climate variations in the South Pacific Convergence Zone region: Geochemistry Geophysics Geosystems, v. 6.

Boiseau, M., Juillet-Leclerc, A., Yiou, P., Salvat, B., Isdale, P., and Guillaume, M., 1998, Atmospheric and oceanic evidences of El Nino Southern Oscillation events in the south central Pacific Ocean from coral stable isotopic records over the last 137 years: Paleoceanography, v. 13, no. 6, p. 671-685.

Charles, C. D., Cobb, K., Moore, M. D., and Fairbanks, R. G., 2003, Monsoon-tropical ocean interaction in a network of coral records spanning the 20th century: Marine Geology, v. 201, no. 1-3, p. 207-222.

Clement, A. C., Seager, R., Cane, M. A., and Zebiak, S. E., 1996, An ocean dynamical thermostat: Journal of Climate, v. 9, no. 9, p. 2190-2196.

Cobb, K. M., Charles, C. D., Cheng, H., and Edwards, R. L., 2003, El Niño/Southern Oscillation and tropical Pacific climate during the last millennium: Nature, v. 424, no. 6946, p. 271-276.

Cole, J. E., Fairbanks, R. G., and Shen, G. T., 1993, Recent variability in the Southern Oscillation; isotopic results from a Tarawa Atoll coral: Science, v. 260, no. 5115, p. 1790-1793.

Collins, M., An, S.-I., Cai, W., Ganachaud, A., Guilyardi, E., Jin, F.-F., Jochum, M., Lengaigne, M., Power, S., Timmermann, A., Vecchi, G., and Wittenberg, A., 2010, The impact of global warming on the tropical Pacific Ocean and El Nino: Nature Geosci., v. 3, no. 6, p. 391-397.

Conroy, J. L., Overpeck, J. T., and Cole, J. E., 2010, El Niño/Southern Oscillation and changes in the zonal gradient of tropical Pacific sea surface temperature over the last 1.2 ka: PAGES news, v. 18, no. 1.

Conroy, J. L., Restrepo, A., Overpeck, J. T., Steinitz-Kannan, M., Cole, J. E., Bush, M. B., and Colinvaux, P. A., 2009, Unprecedented recent warming of surface temperatures in the eastern tropical Pacific Ocean: Nature Geosci, v. 2, no. 1, p. 46-50.

Cook, E. R., Woodhouse, C. A., Eakin, C. M., Meko, D. M., and Stahle, D. W., 2004, Long-Term Aridity Changes in the Western United States: Science, v. 306, no. 5698, p. 1015-1018.

Corrège, T., 2006, Sea surface temperature and salinity reconstruction from coral geochemical tracers: Palaeogeography Palaeoclimatology Palaeoecology, v. 232, no. 2-4, p. 408-428.

Cravatte, S., Delcroix, T., Zhang, D. X., McPhaden, M., and Leloup, J., 2009, Observed freshening and warming of the western Pacific Warm Pool: Climate Dynamics, v. 33, no. 4, p. 565-589.

Crowley, T. J., Quinn, T. M., and Hyde, W. T., 1999, Validation of coral temperature calibrations: Paleoceanography, v. 14, no. 5, p. 605-615.

D'Arrigo, R., Cook, E. R., Wilson, R. J., Allan, R., and Mann, M. E., 2005, On the variability of ENSO over the past six centuries: Geophysical Research Letters, v. 32, no. 3, p. 4.

Delcroix, T., Alory, G., Cravatte, S., Corrège, T., and McPhaden, M. J., 2011, A gridded sea surface salinity data set for the tropical Pacific with sample applications (1950-2008): Deep Sea Research Part I: Oceanographic Research Papers, v. 58, no. 1, p. 38-48.

DeLong, K. L., Quinn, T. M., and Taylor, F. W., 2007, Reconstructing twentieth-century sea surface temperature variability in the southwest Pacific: A replication study using multiple coral Sr/Ca records from New Caledonia: Paleoceanography, v. 22, no. 4.

Druffel, E. R. M., 1997, Geochemistry of corals: Proxies of past ocean chemistry, ocean circulation, and climate: Proceedings of the National Academy of Sciences, v. 94, no. 16, p. 8354-8361.

Druffel, E. R. M., and Griffin, S., 1999, Variability of surface ocean radiocarbon and stable isotopes in the southwestern Pacific: Journal of Geophysical Research-Oceans, v. 104, no. C10, p. 23607-23613.

Dunbar, R. B., Wellington, G. M., Colgan, M. W., and Glynn, P. W., 1994, Eastern Pacific sea-surface temperature since 1600 A.D. - The Delta O 18 record of climate variability in Galapagos corals: Paleoceanography, v. 9, no. 2, p. 291-315.

Emile-Geay, J., Cane, M., Seager, R., Kaplan, A., and Almasi, P., 2007, El Nino as a mediator of the solar influence on climate: Paleoceanography, v. 22, no. 3, p. PA3210.

Evans, M. N., Fairbanks, R. G., and Rubenstone, J. L., 1998a, A proxy index of ENSO teleconnections: Nature, v. 394, no. 6695, p. 732-733.

Evans, M. N., Kaplan, A., and Cane, M. A., 1998b, Optimal sites for coral-based reconstruction of global sea surface temperature: Paleoceanography, v. 13, no. 5, p. 502-516.

-, 2000, Intercomparison of coral oxygen isotope data and historical sea surface temperature (SST): Potential for coral-based SST field reconstructions: Paleoceanography, v. 15, no. 5, p. 551-563.

-, 2002, Pacific sea surface temperature field reconstruction from coral delta O-18 data using reduced space objective analysis: Paleoceanography, v. 17, no. 1, p. 13.

Fairbanks, R. G., Evans, M. N., Rubenstone, J. L., Mortlock, R. A., Broad, K., Moore, M. D., and Charles, C. D., 1997, Evaluating climate indices and their geochemical proxies measured in corals: Coral Reefs, v. 16, p. S93-S100.

Felis, T., Suzuki, A., Kuhnert, H., Dima, M., Lohmann, G., and Kawahata, H., 2009, Subtropical coral reveals abrupt early-twentieth-century freshening in the western North Pacific Ocean: Geology, v. 37, no. 6, p. 527-530.

Gagan, M. K., Ayliffe, L. K., Beck, J. W., Cole, J. E., Druffel, E. R. M., Dunbar, R. B., and Schrag, D. P., 2000, New views of tropical paleoclimates from corals: Quaternary Science Reviews, v. 19, no. 1-5, p. 45-64.

Guilderson, T. P., and Schrag, D. P., 1999, Reliability of coral isotope records from the western Pacific warm pool: A comparison using age-optimized records: Paleoceanography, v. 14, no. 4, p. 457-464.

Hendy, E. J., Gagan, M. K., Alibert, C. A., McCulloch, M. T., Lough, J. M., and Isdale, P. J., 2002, Abrupt decrease in tropical Pacific Sea surface salinity at end of Little Ice Age: Science, v. 295, no. 5559, p. 1511-1514.

Kilbourne, K. H., Quinn, T. M., Taylor, F. W., Delcroix, T., and Gouriou, Y., 2004, El Nino-Southern Oscillation-related salinity variations recorded in the skeletal geochemistry of a Porites coral from Espiritu Santo, Vanuatu: Paleoceanography, v. 19, no. 4.

Koutavas, A., 2009, Was ENSO amplified during the Last Glacial Maximum?: Eos Transactions, American Geophysical Union, v. 90, no. 52, p. PP11G-05.

Kuhnert, H., Patzold, J., Hatcher, B., Wyrwoll, K. H., Eisenhauer, A., Collins, L. B., Zhu, Z. R., and Wefer, G., 1999, A 200-year coral stable oxygen isotope record from a high-latitude reef off western Australia: Coral Reefs, v. 18, no. 1, p. 1-12.

Kuhnert, H., Patzold, J., Wyrwoll, K. H., and Wefer, G., 2000, Monitoring climate variability over the past 116 years in coral oxygen isotopes from Ningaloo Reef, Western Australia: International Journal of Earth Sciences, v. 88, no. 4, p. 725-732.

Larkin, N. K., and Harrison, D. E., 2005, On the definition of El Niño and associated seasonal average US weather anomalies: Geophysical Research Letters, v. 32, no. 13, p. 4.

LeGrande, A. N., and Schmidt, G. A., 2006, Global gridded data set of the oxygen isotopic composition in seawater: Geophys. Res. Lett., v. 33, no. 12, p. L12604.

Li, J., Xie, S.-P., Cook, E. R., Huang, G., D'Arrigo, R., Liu, F., Ma, J., and Zheng, X.-T., 2011, Interdecadal modulation of El Niño amplitude during the past millenium: Nature Climate Change, v. 1, p. 114-118.

Linsley, B. K., Dunbar, R. B., Wellington, G. M., and Mucciarone, D. A., 1994, A coral-based reconstruction of intertropical convergence zone variability over Central America since 1707: Journal of Geophysical Research-Oceans, v. 99, no. C5, p. 9977-9994.

Linsley, B. K., Kaplan, A., Gouriou, Y., Salinger, J., Demenocal, P. B., Wellington, G. M., and Howe, S. S., 2006, Tracking the extent of the South Pacific Convergence Zone since the early 1600s: Geochemistry Geophysics Geosystems, v. 7.

Linsley, B. K., Messier, R. G., and Dunbar, R. B., 1999, Assessing between-colony oxygen isotope variability in the coral Porites lobata at Clipperton Atoll: Coral Reefs, v. 18, no. 1, p. 13-27.

Linsley, B. K., Ren, L., Dunbar, R. B., and Howe, S. S., 2000, El Niño Southern Oscillation (ENSO) and decadal-scale climate variability at 10 degrees N in the eastern Pacific from 1893 to 1994: A coral-based reconstruction from Clipperton Atoll: Paleoceanography, v. 15, no. 3, p. 322-335.

Linsley, B. K., Wellington, G. M., Schrag, D. P., Ren, L., Salinger, M. J., and Tudhope, A. W., 2004, Geochemical evidence from corals for changes in the amplitude and spatial pattern of South Pacific interdecadal climate variability over the last 300 years: Climate Dynamics, v. 22, no. 1, p. 1-11.

Lukas, R., and Lindstrom, E., 1991, The mixed layer of the western equatorial Pacific Ocean: J. Geophys. Res.-Oceans, v. 96, p. 3343-3357.

Mann, M. E., Cane, M. A., Zebiak, S. E., and Clement, A., 2005, Volcanic and solar forcing of the tropical Pacific over the past 1000 years: Journal of Climate, v. 18, no. 3, p. 447-456.

McGregor, S., Timmermann, A., and Timm, O., 2010, A unified proxy for ENSO and PDO variability since 1650: Climate of the Past, v. 6, no. 1, p. 1-17.

Moy, C. M., Seltzer, G. O., Rodbell, D. T., and Anderson, D. M., 2002, Variability of El Nino/Southern Oscillation activity at millennial timescales during the Holocene epoch: Nature, v. 420, no. 6912, p. 162-165.

Okumura, Y. M., and Deser, C., 2010, Asymmetry in the Duration of El Niño and La Niña: Journal of Climate, v. 23, no. 21, p. 5826-5843.

Oppo, D. W., Rosenthal, Y., and Linsley, B. K., 2009, 2,000-year-long temperature and hydrology reconstructions from the Indo-Pacific warm pool: Nature, v. 460, no. 7259, p. 1113-1116.

Ortlieb, L., 2000, The documented historical record of El Nino events in Peru: An update of the Quinn record (sixteenth through nineteenth centuries), *in* Diaz, H. F., and Markgraf, V., eds., El Nino and the Southern Oscillation: Multiscale Variability and Global and Regional Impacts: Cambridge, UK, Cambridge University Press.

Quinn, T. M., Crowley, T. J., Taylor, F. W., Henin, C., Joannot, P., and Join, Y., 1998, A multicentury stable isotope record from a New Caledonia coral: Interannual and decadal sea surface temperature variability in the southwest Pacific since 1657 A.D.: Paleoceanography, v. 13, no. 4, p. 412-426.

Quinn, T. M., and Sampson, D. E., 2002, A multiproxy approach to reconstructing sea surface conditions using coral skeleton geochemistry: Paleoceanography, v. 17, no. 4, p. 1062.

Quinn, T. M., Taylor, F. W., and Crowley, T. J., 2006, Coral-based climate variability in the Western Pacific Warm Pool since 1867: J. Geophys. Res.-Oceans, v. 111, no. C11, p. C11006.

Rasmusson, E. M., and Carpenter, T. H., 1982, Variations in tropical sea-surface temperature and surface wind fields associated with the Southern Oscillation/El Nino: Monthly Weather Review, v. 110, no. 5, p. 354-384.

Rayner, N. A., Parker, D. E., Horton, E. B., Folland, C. K., Alexander, L. V., Rowell, D. P., Kent, E. C., and Kaplan, A., 2003, Global analyses of sea surface temperature, sea ice, and night marine air temperature since the late nineteenth century: Journal of Geophysical Research-Atmospheres, v. 108, no. D14, p. 37.

Ropelewski, C. F., and Halpert, M. S., 1987, Global and regional scale precipitation patterns associated with the El Niño Southern Oscillation: Monthly Weather Review, v. 115, no. 8, p. 1606-1626.

Schrag, D. P., 1999, Rapid analysis of high-precision Sr/Ca ratios in corals and other marine carbonates: Paleoceanography, v. 14, no. 2, p. 97-102.

Singh, A., and Delcroix, T., 2011, Estimating the effects of ENSO upon the observed freshening trends of the western tropical Pacific Ocean: Geophys. Res. Lett., v. 38, no. 21, p. L21607.

Stahle, D. W., D'Arrigo, R. D., Krusic, P. J., Cleaveland, M. K., Cook, E. R., Allan, R. J., Cole, J. E., Dunbar, R. B., Therrell, M. D., Gay, D. A., Moore, M. D., Stokes, M. A., Burns, B. T., Villanueva-Diaz, J., and Thompson, L. G., 1998, Experimental

dendroclimatic reconstruction of the Southern Oscillation: Bulletin of the American Meteorological Society, v. 79, no. 10, p. 2137-2152.

Steinhilber, F., Abreu, J. A., Beer, J., Brunner, I., Christl, M., Fischer, H., Heikkilä, U., Kubik, P. W., Mann, M., McCracken, K. G., Miller, H., Miyahara, H., Oerter, H., and Wilhelms, F., 2012, 9,400 years of cosmic radiation and solar activity from ice cores and tree rings: Proceedings of the National Academy of Sciences, v. 109, no. 16, p. 5967-5971.

Steinhilber, F., Beer, J., and Fröhlich, C., 2009, Total solar irradiance during the Holocene: Geophys. Res. Lett., v. 36, no. 19, p. L19704.

Stevenson, S., Fox-Kemper, B., Jochum, M., Neale, R., Deser, C., and Meehl, G., 2012, Will There Be a Significant Change to El Niño in the Twenty-First Century?: Journal of Climate, v. 25, no. 6, p. 2129-2145.

Thompson, D. M., Ault, T. R., Evans, M. N., Cole, J. E., and Emile-Geay, J., 2011, Comparison of observed and simulated tropical climate trends using a forward model of coral δ18O: Geophys. Res. Lett., v. 38, no. 14, p. L14706.

Thompson, L. G., Mosley-Thompson, E., Davis, M. E., Lin, P. N., Henderson, K. A., Coledai, J., Bolzan, J. F., and Liu, K. B., 1995, Late-glacial stage and Holocene tropical ice core records from Huascaran, Peru: Science, v. 269, no. 5220, p. 46-50.

Tierney, J. E., Oppo, D. W., Rosenthal, Y., Russell, J. M., and Linsley, B. K., 2010, Coordinated hydrological regimes in the Indo-Pacific region during the past two millennia: Paleoceanography, v. 25, no. 1, p. PA1102.

Torrence, C., and Compo, G. P., 1998, A practical guide to wavelet analysis: Bulletin of the American Meteorological Society, v. 79, no. 1, p. 61-78.

Trenberth, K. E., 1997, The definition of El Niño: Bulletin of the American Meteorological Society, v. 78, no. 12, p. 2771-2777.

Trenberth, K. E., and Tepaniak, D. P., 2001, Indices of El Nino evolution: Journal of Climate, v. 14, no. 8, p. 1697-1701.

Tudhope, A. W., Chilcott, C. P., McCulloch, M. T., Cook, E. R., Chappell, J., Ellam, R. M., Lea, D. W., Lough, J. M., and Shimmield, G. B., 2001, Variability in the El Niño - Southern Oscillation through a glacial-interglacial cycle: Science, v. 291, no. 5508, p. 1511-1517.

Tziperman, E., Stone, L., Cane, M. A., and Jarosh, H., 1994, El Niño Chaos: Overlapping of Resonances Between the Seasonal Cycle and the Pacific Ocean-Atmosphere Oscillator: Science, v. 264, no. 5155, p. 72-74.

Urban, F. E., Cole, J. E., and Overpeck, J. T., 2000, Influence of mean climate change on climate variability from a 155-year tropical Pacific coral record: Nature, v. 407, no. 6807, p. 989-993.

Vecchi, G. A., and Soden, B. J., 2007, Global warming and the weakening of the tropical circulation: Journal of Climate, v. 20, no. 17, p. 4316-4340.

Wilson, R., Cook, E., D'Arrigo, R., Riedwyl, N., Evans, M. N., Tudhope, A., and Allan, R., 2010, Reconstructing ENSO: the influence of method, proxy data, climate forcing and teleconnections: Journal of Quaternary Science, v. 25, no. 1, p. 62-78.

Wilson, R., Tudhope, A., Brohan, P., Briffa, K., Osborn, T., and Tett, S., 2006, Two-hundred-fifty years of reconstructed and modeled tropical temperatures: Journal of Geophysical Research-Oceans, v. 111, no. C10, p. 13.

Wittenberg, A. T., 2009, Are historical records sufficient to constrain ENSO simulations?: Geophys. Res. Lett., v. 36, p. L12702.

Zhang, P. Z., Cheng, H., Edwards, R. L., Chen, F. H., Wang, Y. J., Yang, X. L., Liu, J., Tan, M., Wang, X. F., Liu, J. H., An, C. L., Dai, Z. B., Zhou, J., Zhang, D. Z., Jia, J. H., Jin, L. Y., and Johnson, K. R., 2008, A test of climate, sun, and culture relationships from an 1810-year Chinese cave record: Science, v. 322, no. 5903, p. 940-942.

Vita

Kelly Ann Hereid attended Eureka High School, in Eureka, Missouri. In 2003 she entered Carleton College in Northfield, Minnesota. She received the degree of Bachelor of Arts from Carleton College in June, 2007, majoring in biology and geology. In August, 2007, she entered the Graduate School at The University of Texas at Austin in the Jackson School of Geosciences. She began work as a research scientist in catastrophe modeling with ACE Tempest Re in Stamford, Connecticut in August, 2012.

Permanent Address: 330 E 39th St. Apt. 34K, New York, NY 10016

This manuscript was typed by the author.